

Determination of the Anomalous Chiral Coefficients of order p^6

Master of Science Thesis

author: Olof Strandberg

advisor: Johan Bijnens

Department of Theoretical Physics, Lund University
Sölvegatan 14A, S22362 Lund, Sweden

Abstract

Symmetries affected by the anomaly do not survive quantization and cannot be understood classically. They are of fundamental importance and offer an opportunity of expanding the theoretical framework. We examine the theory of the anomalous sector, starting from lowest order Chiral Perturbation Theory (ChPT), leading up to the construction of the recently developed Lagrangian of $\mathcal{O}(p^6)$ describing anomalous processes. This Lagrangian contains a set of chiral coefficients that must be determined phenomenologically. Using currently available experimental data, we fit as many of these coefficients as possible. The results of the ChPT treatment are then used to test the validity of the two main alternative models employed in the anomalous sector - Vector Meson Dominance (VMD) and the constituent Chiral Quark Model (CQM).

Contents

1	Introduction	2
2	Symmetries	3
2.1	Chiral Symmetry	3
2.2	Non-linear Realization of Chiral Symmetry	4
3	Effective Quantum Field Theories (EQFT)	5
4	Chiral Perturbation Theory (ChPT)	6
4.1	Lowest Order Effective Lagrangian	6
4.2	Power Counting	7
4.3	Vacuum Expectation Values and Masses	8
4.4	The $\mathcal{O}(p^4)$ effective action	9
4.5	Anomalous Processes	9
5	η' (958)	10
6	$\eta_8 - \eta_0$ mixing	11
7	Anomalies	11
7.1	Classical vs. Quantum Symmetries	12
7.2	The $U(1)_A$ Axial Anomaly	13
8	The Wess-Zumino-Witten (WZW) Anomaly Action	14
8.1	Anomalous Terms	14
8.2	Example of Calculation	16
9	Loops and Renormalization	17
9.1	Power Counting	18
9.2	Infinite parts	18
9.3	Meson One-Loop Corrections	19
10	Anomalous Lagrangian of $\mathcal{O}(p^6)$	19
10.1	Construction of the Effective Action	20
10.2	Infinite parts	21
10.3	Example of Calculation	21
11	Models for the Chiral Coefficients	22
11.1	Vector Meson Dominance (VMD)	22
11.2	Chiral Constituent Quark Model (CQM)	23
12	Results	24
12.1	Combining Amplitudes	24
12.2	Theoretical Quantum Field Calculations	25
12.3	Experimental Comparison	27
12.3.1	$\pi^0/\eta \rightarrow \gamma\gamma^*$	27
12.3.2	$\pi^+/K^+ \rightarrow \gamma e^+\nu$	29

12.3.3	$\gamma\pi^0\pi^+\pi^-$	29
12.3.4	$\eta\gamma\pi^+\pi^-$	30
12.3.5	$K^+ \rightarrow \pi^+\pi^-e^+\nu$	30
12.4	VMD Comparison	32
12.5	CQM Comparison	34
13	Conclusions & Outlook	37
A	<i>One-loop Corrections</i>	40
B	<i>CQM Lagrangians</i>	42

1 Introduction

In high energy QCD, we have asymptotic freedom and scattering can be calculated in a power series expansion in the strong coupling constant. The non-perturbative effects are determined phenomenologically in the form of structure and fragmentation functions. Predictions take the form of relations between amplitudes parametrized by α_s and the structure functions.

In low energy QCD, the predictions are relations between amplitudes with a structure determined by symmetry constraints, parametrized by empirically determined coefficients. The power series expansion in α_s is replaced by an expansion in the low energy. Heavy fields of the high energy region can be integrated out and their effect is consequently encoded in the coefficients of the low energy effective theory. Proceeding up to $\mathcal{O}(p^6)$ in ChPT, we are confronted with a large number of empirical parameters. In principle, QCD should be able to predict these parameters, as well as the structure functions appearing in the chiral Lagrangian. No rigorous derivation exists up to date. The combined use of tentative models and phenomenological knowledge provides us with insight of the physics leading to the chiral Lagrangian. The aim of this thesis is to solve for as many low energy chiral coefficients as possible by making use of the available experimental data in the form of widths, slopes and form factors.

Classically conserved currents that are affected by the anomaly do not survive quantization. To evaluate the ensuing effects, it is necessary to employ a more rigorous analysis, taking quantum corrections into account. The effect of the anomaly in the chiral Lagrangian framework was first analyzed by Wess and Zumino [1], who realized that the result could not be expressed in a local effective Lagrangian. Their result, in the form of a Taylor series expansion, was later given an elegant geometrical interpretation by Witten [2].

So far most articles treating anomalous processes quote the leading order amplitudes and meson one-loop corrections. Higher order contributions are then estimated using models like Vector Meson Dominance (VMD) or the more recently developed chiral Constituent Quark Model (CQM). In this thesis we will instead test the validity of VMD and CQM by comparing with the results of the experimentally fixed chiral $\mathcal{O}(p^6)$ coefficients.

2 Symmetries

2.1 Chiral Symmetry

Apart from the more obvious symmetries of the standard model, such as the gauge symmetries $SU(3)_c \times SU(2)_L \times U(1)_Y$, there exist global vector symmetries like the fermion number symmetries, the isospin symmetry, and the less accurate $SU(3)$ flavor symmetry. The flavor symmetries are valid if the masses of the quarks included by the symmetry are set equal. Therefore, the isospin symmetry is broken by the up-down quark mass difference, as well as by electromagnetic and weak interactions. By imposing the considerably stricter condition, $m_q = 0$, so called chiral symmetries arise. Since there are no longer any mass terms to couple fields of differing chirality, the fields are invariant under separate left- and right-handed transformations. The QCD Lagrangian in the massless limit is given by

$$\begin{aligned}\mathcal{L}_{QCD}^{m=0} &= \sum_{q=u,d,s} \bar{q} \gamma^\mu \left(i \partial_\mu - g_s \frac{\lambda_a}{2} G_\mu^a \right) q - \frac{1}{4} G_{\mu\nu}^a G_a^{\mu\nu} \\ &= \bar{\psi}_L \not{D} \psi_L + \bar{\psi}_R \not{D} \psi_R - \frac{1}{4} G_{\mu\nu}^a G_a^{\mu\nu}\end{aligned}\quad (1)$$

where $\psi_{R,L} = \frac{1}{2}(1 \pm \gamma_5) \psi = P_{R,L} \psi$ are the chiral projections of the column vector containing the relevant quark fields (u, d for chiral $SU(2)$ and u, d, s for chiral $SU(3)$). Taking $m_u = m_d = 0$, the QCD Lagrangian is invariant under chiral rotations of the fields

$$\psi_L \rightarrow e^{-i\vec{\theta}_L \cdot \vec{\tau}} \psi_L \equiv g_L \psi_L \quad (2)$$

$$\psi_R \rightarrow e^{-i\vec{\theta}_R \cdot \vec{\tau}} \psi_R \equiv g_R \psi_R \quad (3)$$

where $\{\tau^i = \frac{1}{2}\sigma^i\}$ ($i = 1, 2, 3$) are the Pauli matrices and $\{\theta_{L,R}^i\}$ are the components of an arbitrary constant vector. The chiral $SU(2)$ invariance is referred to as the direct product of the left- and right-handed chiral transformation groups, $SU(2)_L \times SU(2)_R$. This symmetry is easily extended to include the strange quark, substituting the Pauli matrices for the Gell-Mann 3×3 $SU(3)$ matrices $\frac{1}{2}\{\lambda^a\}$ ($a = 1, \dots, 8$). In eq. (1), we also find the vector $U(1)_V$ and the axial $U(1)_A$ invariances

$$\psi \rightarrow e^{i\theta} \psi \quad (4)$$

$$\psi \rightarrow e^{i\theta\gamma_5} \psi \quad (5)$$

So apart from the normal $SU(3)_c$ color gauge and discrete symmetries, the chiral QCD Lagrangian also has the global invariance

$$U(1)_A \times U(1)_V \times SU(3)_R \times SU(3)_L \quad (6)$$

where there are now separate invariances under $SU(3)_L$ and $SU(3)_R$, for the three massless quarks. The $U(1)_V$ is conserved, ensuring baryon number conservation. The axial $U(1)_A$ current is not conserved in the full quantum theory, and is explicitly broken by the Abelian anomaly.

Let G be the direct product group of the left- and right-handed chiral transformations: $\psi_{L,R} \rightarrow g_{L,R} \psi_{L,R}$, $g_{L,R} \in G$. Then (1) is invariant under G . However, the QCD vacuum structure does not share this invariance. The effect of a non-vanishing quark condensate,

i.e. a non-zero vacuum expectation value $\langle 0 | \bar{\psi} \psi | 0 \rangle \neq 0$, is the spontaneous breaking of the axial part of G . Spontaneous (dynamic) symmetry breaking is said to occur whenever the symmetry of the Lagrangian is not shared by the ground (vacuum) state. For G we have

$$SU(3)_L \times SU(3)_R \rightarrow SU(3)_{V=L+R} \quad (7)$$

where $SU(3)_V \equiv H$ is the remaining unbroken subgroup of simultaneous transformations of differing chirality. According to the Goldstone theorem, whenever a global continuous symmetry is broken, massless so called Goldstone (GS) bosons appear. Since it is the axial part that is broken, the resulting GS bosons are pseudoscalars. An $SU(n)$ matrix has $n^2 - 1$ parameters (due to the unitarity and determinant constraints). The matrix of the coset space $G/H = SU(3)_L \times SU(3)_R / SU(3)_V$, used to parametrize the GS bosons is an $SU(3)$ isomorphism, also represented by a 3×3 matrix, containing 8 pseudoscalars. These are the light pseudoscalar mesons of the low energy spectrum: $\pi^\pm, \pi^0, K^\pm, K^0, \bar{K}^0$ and η . If we instead would have chosen to focus on the up and down quark, setting $m_u = m_d = 0$, the resulting spectrum would have been described by the 2×2 $SU(2)$ matrices, containing the $2^2 - 1 = 3$ pions: π^+, π^- and π^0 .

The only visible symmetry in hadronic states is $U(1)_V \times SU(3)_V$. The effect of $U(1)_V$ can only be seen by including the (non-trivially transforming) baryon fields in the effective Lagrangian.

The proof of the breaking of the axial symmetry lies in the predictions it makes, and can be produced by Monte Carlo lattice gauge techniques. The main motivation for the existence of this mechanism lies in its phenomenological success and theoretical consistency.

GS bosons are massless, but the physical particles are clearly not. However, the quark masses are small compared to the breaking scale of the chiral symmetry ($m_{u,d,s} < \Lambda_\chi \sim 1\text{GeV}$). This enables us to treat them as a small perturbation, and we can include the quark masses in the Lagrangian as external scalar fields. The inclusion of mass terms will mean the explicit breaking of G . Perturbational treatment is supported by the relatively small size of the pseudoscalar masses compared to the hadronic scale ($m_\pi^2/m_\rho^2 \sim 0.03$ for $SU(2)$ and $m_K^2/m_\rho^2 \sim 0.3$ for $SU(3)$).

The task at hand is to construct a chiral invariant low energy effective quantum theory with the GS bosons as dynamic fields.

2.2 Non-linear Realization of Chiral Symmetry

Before we can construct an invariant Lagrangian, we must examine the transformation properties of the Goldstone boson degrees of freedom. G is a compact connected Lie group, that is dynamically broken into the subgroup H . The coordinates of the coset space $G/H = SU(3)_L \times SU(3)_R / SU(3)_{L+R}$ are the remaining degrees of freedom describing the system, i.e. the GS bosons. The transformation of an element parametrized by the GS bosons under G

$$gu(\xi_i) \rightarrow u(\xi'_i)h(\xi_i, g) \quad ; g \in G, h \in H$$

is non-linear in nature since the generators of H and G/H do not commute. What we want is to construct operators that transform linearly under G , that is to say are chiral invariant. To this we then add the explicitly symmetry breaking light quark masses. Linear operators can be constructed by starting from projections onto the transformation subgroup H . As shown by Callan, Coleman, Wess & Zumino [4], this is the most general way of constructing

operators linear under G in terms of the GS bosons. A given field ψ , transforming linearly under H , transforms under G as $\psi \rightarrow h(g, \xi_i) \psi h^{-1}(g, \xi_i)$. This means that all products of type $(u, u^\dagger) \cdot \psi \cdot (u, u^\dagger)$ will transform linearly under G . For a more technical treatment of how this can be done the reader is referred to [5].

From the derivative of u and u^\dagger we can define the Hermitian operator u_μ and the covariant derivative ∇_μ , both of which transform linearly under G .

$$u_\mu = i(u^\dagger \partial_\mu u - u \partial_\mu u^\dagger) \quad (8)$$

$$\nabla_\mu \psi = \partial_\mu \psi - [\Gamma_\mu, \psi] \quad ; \Gamma_\mu = \frac{1}{2} (u^\dagger \partial_\mu u + u \partial_\mu u^\dagger) \quad (9)$$

These can be used as building blocks to construct the linear operators. To get the correct behavior in the low energy limit, it is necessary to have derivative interactions. This is not a problem since the Goldstone fields can easily be rewritten to accommodate this soft behavior. The invariant term is realized by taking the trace in flavor space, denoted by $\langle \dots \rangle$.

The parametrization of the coset space is not unique. It can be shown that S -matrix elements are invariant under a field redefinition $\psi = \phi F(\phi)$, where $F(0) = 1$. The power counting depends on the number of derivatives, which is unchanged by the redefinition, so the results are representation independent, order by order. It is advantageous to use an exponential parametrization in 3×3 flavor space.

$$u^2 = U = e^{i \frac{\sqrt{2}}{F} M} \quad (10)$$

where F is a dimensional constant of same dimension as M - the Goldstone boson matrix

$$M = \frac{1}{\sqrt{2}} \sum_{i=1}^8 \lambda_i \phi^i = \begin{pmatrix} \frac{\pi^0}{\sqrt{2}} + \frac{\eta_8}{\sqrt{6}} & \pi^+ & K^+ \\ \pi^- & -\frac{\pi^0}{\sqrt{2}} + \frac{\eta_8}{\sqrt{6}} & K^0 \\ K^- & \bar{K}^0 & -\frac{2\eta_8}{\sqrt{6}} \end{pmatrix} \quad (11)$$

where λ_i are the Gell-Mann $SU(3)$ matrices, ϕ^i the Goldstone fields and η_8 denotes the octet component of η (see section on η_8 - η_0 mixing).

3 Effective Quantum Field Theories (EQFT)

QCD is a gauge theory describing the interactions of quarks and gluons. Below Λ_χ it becomes highly non-perturbative. As a consequence, we can no longer use the partonic degrees of freedom to describe it. The effective chiral Lagrangian approach makes use of the very simple low energy spectrum of light pseudoscalar mesons: $\pi^\pm, \pi^0, K^0, \bar{K}^0, K^\pm$ and η , as dynamic fields describing the theory. Considering the weak nature of interactions amongst and between the light mesons and nucleons, the perturbative approach can be reinstated by simply transforming to the relevant degrees of freedom, i.e. the light pseudoscalar mesons. This is the principle for all effective quantum field theories. At a given energy, only certain degrees of freedom are relevant in describing the theory. The non-relevant degrees of freedom can be integrated out, and their effect is consequently encoded in the coefficients of the effective theory. All quantum field theories can be regarded as EQFTs. However, they differ in their degree of renormalizability. Since the theory is valid only below a given intrinsic scale parameter Λ , we can expand amplitudes in terms of E/Λ , and require a finite number of counterterms in order to regularize at any $\mathcal{O}(E^n/\Lambda^n)$.

If we want to be able to study relevant physical processes, the needed external source fields must enter the Lagrangian. These are conveniently included in a chiral invariant way. They take the form of external scalar (s), pseudoscalar (p), right- (r_μ) and left-handed (ℓ_μ) 3×3 matrix source functions.

$$\mathcal{L}_{QCD} = \dots - \bar{\psi} \gamma_\mu P_L \ell^\mu \psi - \bar{\psi} \gamma_\mu P_R r^\mu \psi - \bar{\psi}_L (s + ip) \psi_R - \bar{\psi}_R (s - ip) \psi_L \quad (12)$$

Here we see that the quark mass matrix $s = m = \text{diag}(m_u, m_d, m_s)$ explicitly breaks the left and right chiral symmetries. The electroweak gauge fields enter through ℓ_μ and r_μ .

The low energy effective action for the GS bosons is a functional of external sources. We obtain the QCD connection by considering the effect of the sources.

$$e^{iZ(\ell_\mu, r_\mu, s, p)} = \int [d\bar{\psi}][d\psi][dA_\mu^a] e^{i \int d^4x \mathcal{L}_{QCD}(\psi, \bar{\psi}, A_\mu^a, \ell_\mu, r_\mu, s, p)} \quad (13)$$

Only the GS bosons are the relevant degrees of freedom at low energies, so in integrating out the heavy fields (thereby absorbing them into coefficients) and transforming to the GS system gives

$$e^{iZ(\ell_\mu, r_\mu, s, p)} = \int [dU] e^{i \int d^4x \mathcal{L}_{eff}(U, \ell_\mu, r_\mu, s, p)} \quad (14)$$

4 Chiral Perturbation Theory (ChPT)

Chiral Perturbation Theory is an EQFT describing hadronic interactions in the low energy limit of the standard model. It is valid below the breaking scale of chiral symmetry, i.e. for energies $\ll 1\text{GeV} \sim \Lambda_\chi$. The chiral theory successfully describes the mesonic sector, and has also been extended to other fields such as heavy quark and bound state dynamics. ChPT is the evolved form of Partial Conservation of the Axial current (PCAC) and current algebra techniques.

4.1 Lowest Order Effective Lagrangian

To obtain terms that are invariant under both chiral and Lorentz symmetries, at least two derivatives of u or u^\dagger must be present. In the absence of external fields there is only one term of $\mathcal{O}(p^2)$

$$\mathcal{L}_2^{(0)} = \frac{F^2}{4} \left\langle \partial_\mu U \partial^\mu U^\dagger \right\rangle \quad (15)$$

where the coupling is set to reproduce the correct kinetic term. Adding source functions coupled to their associated currents (following Gasser & Leutwyler [6]), as in eq. (12), we find the global symmetries (6) implying the following invariances:

$$\psi \xrightarrow{U(1)_V} e^{i\varepsilon} \psi \quad (16)$$

$$\psi \xrightarrow{U(1)_A} e^{i\gamma_5 \varepsilon} \psi \quad (17)$$

$$\psi \xrightarrow{G} (g_L P_L + g_R P_R) \psi \quad ; g_{R,L} = e^{-i\vec{\theta}_{L,R} \cdot \vec{\lambda}/2} \in G \quad (18)$$

$$\ell_\mu = v_\mu - a_\mu \xrightarrow{G} g_L \ell_\mu g_L^{-1} \quad (19)$$

$$r_\mu = v_\mu + a_\mu \xrightarrow{G} g_R r_\mu g_R^{-1} \quad (20)$$

$$s \pm ip \xrightarrow{G} g_{R,L} (s \pm ip) g_{L,R}^{-1} \quad (21)$$

These can all be made local by adding terms to the transformation of the vector fields ℓ_μ, r_μ .

$$\begin{aligned} & \xrightarrow{U(1)_V} \begin{Bmatrix} \ell_\mu - \partial_\mu \varepsilon \\ r_\mu - \partial_\mu \varepsilon \end{Bmatrix} \\ \left. \begin{matrix} \ell_\mu \\ r_\mu \end{matrix} \right\} & \xrightarrow{U(1)_A} \begin{Bmatrix} \ell_\mu + \partial_\mu \varepsilon \\ r_\mu - \partial_\mu \varepsilon \end{Bmatrix} \\ & \xrightarrow{G} \begin{Bmatrix} g_L (\ell_\mu + i\partial_\mu) g_L^{-1} \\ g_R (r_\mu + i\partial_\mu) g_R^{-1} \end{Bmatrix} \end{aligned} \quad (22)$$

The pseudoscalar source is not relevant for the processes considered here (it appears for example in the Higgs-sector), and the scalar field is set to the light quark mass matrix. (12) shows that the s field transforms non-trivially under G , explicitly breaking the chiral symmetry. But because the light quark masses are much smaller than the chiral breaking scale, we still have approximate chiral symmetry.

Comparing with the SM Lagrangian we can make the identifications

$$v_\mu \rightarrow -eQA_\mu - \frac{g}{2\sqrt{2}} (T_+ W_\mu^+ + T_- W_\mu^-) \quad (23)$$

$$a_\mu \rightarrow \frac{g}{2\sqrt{2}} (T_+ W_\mu^+ + T_- W_\mu^-) \quad (24)$$

where the neutral weak gauge fields have been omitted, since their contribution will be strongly suppressed by the heavy Z^0 mass. Q is the electric charge matrix $Q = \frac{1}{3} \text{diag}(2, -1, -1)$ and

$$T_+ = \begin{pmatrix} 0 & V_{ud} & V_{us} \\ 0 & 0 & 0 \\ 0 & 0 & 0 \end{pmatrix} \quad (25)$$

and its Hermitian conjugate T_- contain elements from the weak mixing matrix.

The non-abelian field strength tensors are given by

$$F_L^{\mu\nu} = \partial^\mu \ell^\nu - \partial^\nu \ell^\mu - i[\ell^\mu, \ell^\nu] \quad (26)$$

$$F_R^{\mu\nu} = \partial^\mu r^\nu - \partial^\nu r^\mu - i[r^\mu, r^\nu] \quad (27)$$

Local invariance is maintained by replacing ∂_μ in (15) by the covariant derivative D_μ .

$$\partial_\mu U \rightarrow D_\mu U = \partial_\mu U - ir_\mu U + iU \ell_\mu \quad (28)$$

4.2 Power Counting

To organize our results we must examine how powers in the chiral expansion are counted, so that we can assign them to the Lagrangian of appropriate order. It is the order expansion that makes the whole approach useful. If we assign $\partial_\mu u$ and a_μ, v_μ the same power counting, $D_\mu U$ becomes a first order homogeneous term in the derivative expansion. We then have $U \sim \mathcal{O}(p^0)$, $a_\mu, v_\mu, u_\mu \sim \mathcal{O}(p^1)$, $s, p, F_{L,R}^{\mu\nu} \sim \mathcal{O}(p^2)$. The lowest order Lagrangian including external sources is given by:

$$\mathcal{L}_2 = \frac{F^2}{4} \left\langle D_\mu U D^\mu U^\dagger + \chi U^\dagger + U \chi^\dagger \right\rangle \quad (29)$$

where $\chi = 2B_0(s + ip)$, and B_0 is a constant related to the vacuum expectation value $\langle \bar{\psi}\psi \rangle_0$. The coupling F is can be identified with the pion decay constant F_π .

4.3 Vacuum Expectation Values and Masses

The axial symmetry is a hidden symmetry, meaning that it is dynamically broken - the invariance of the Lagrangian is not shared by the vacuum state. It can be seen that the vacuum state does not transform separately under left and right chiral transformations, as it couples ψ_L with ψ_R .

$$\begin{aligned}\langle 0 | \bar{\psi} \psi | 0 \rangle &= \langle 0 | \bar{\psi} (P_L + P_R)^2 \psi | 0 \rangle \\ &= \langle 0 | \bar{\psi}_L \psi_R | 0 \rangle + \langle 0 | \bar{\psi}_R \psi_L | 0 \rangle\end{aligned}\quad (30)$$

where we have used the projection operator properties and

$$\bar{\psi}_{L,R} = (P_{L,R} \psi)^\dagger \gamma^0 = \psi^\dagger P_{L,R} \gamma^0 = \bar{\psi} P_{R,L} \quad (31)$$

(by the commutation relations for the gamma matrices). In a world of massless quarks, the cost of producing a quark-antiquark pair with total angular momentum and momentum zero, is small. The vacuum can be seen as containing a condensate of $q\bar{q}$ pairs with strong attractive interactions. Mixing of chirality (30) implies that up and down quarks can acquire an effective (constituent) mass by moving through and interacting with the vacuum (see for example [7]).

We can evaluate current matrix elements by differentiating the classical action $S_2 = \int d^4x \mathcal{L}_2$ with respect to external sources. This gives the lowest order result:

$$\langle 0 | \bar{d} \gamma^\mu \gamma_5 u | \pi^+ (p) \rangle = \langle 0 | \frac{\delta S_2}{\delta a_\mu} | \pi^+ (p) \rangle = i\sqrt{2} F p^\mu \quad (32)$$

$$\langle 0 | \bar{\psi} \psi | 0 \rangle = - \langle 0 | \frac{\delta S_2}{\delta s} | 0 \rangle = -F^2 B_0 \quad (33)$$

From the definition of the pion decay constant,

$$i\sqrt{2} F_\pi p^\mu = \langle 0 | \bar{d} \gamma^\mu \gamma_5 u | \pi^+ (p) \rangle$$

we see that to lowest order we can make the identification $F = F_\pi$. Relations (32) & (33) are only valid in the chiral limit, and are subject to corrections of order $\mathcal{O}(m_q)$. (33) relates B_0 to the vacuum expectation value.

The combination $B_0 m_q$ is experimentally determinable. The reason for identifying $\mathcal{O}(m_q) \sim \mathcal{O}(p^2)$ becomes clear if we expand (29) to second order in meson fields. We then get the relations

$$M_{\pi^+}^2 = B_0 (m_u + m_d) \quad (34)$$

$$M_{K^+}^2 = B_0 (m_u + m_s) \quad (35)$$

$$M_{K^0}^2 = B_0 (m_d + m_s) \quad (36)$$

$$M_{\eta_8}^2 = \frac{1}{3} B_0 (m_u + m_d + 4m_s) \quad (37)$$

By elimination we obtain the Gell-Mann-Okubo consistency relation for the GS bosons $3M_{\eta_8}^2 = 4M_K^2 - M_\pi^2$ [8]. This is reasonably¹ well satisfied using $m_u \simeq m_d$ and $M_{\eta_8} \simeq M_\eta$ (see η mixing). For higher mass resonances both linear and quadratic mass formulas give acceptable relations [9]. This is because to first order in symmetry breaking we have $\delta(m^2) =$

¹Putting in the numbers we find that we're off by approximately 20 MeV, but if we instead use linear relations, the numbers get worse (~ 70 MeV).

$(m_0 + \delta m)^2 - m_0^2 = 2m_0\delta m + \dots$ But when expanding around a massless limit m and m^2 distinction becomes important. In the normalized effective theory, the pion mass prediction is

$$m_\pi^2 = (m_u + m_d) B_0 + (m_u + m_d)^2 C_0 + \dots \quad (38)$$

However, there is no symmetry constraint to force the renormalized parameter B_0 to zero, so the squared pion mass is (mostly) linear in the symmetry breaking quark masses.

4.4 The $\mathcal{O}(p^4)$ effective action

Listing all possible operators invariant under discrete and continuous symmetries, transforming linearly, we can construct the tree-level effective chiral action of order p^4 . The number of terms can be reduced to a minimum using the equations of motion for $\mathcal{O}(p^2)$, partial integration, the unitarity of U and $SU(n)$ n -depending trace identities. \mathcal{L}_4 for $SU(3)$ was first determined by Gasser and Leutwyler [6] and is given by

$$\begin{aligned} \mathcal{L}_4 = & L_1 \langle D_\mu U D^\mu U^\dagger \rangle^2 + L_2 \langle D_\mu U D_\nu U^\dagger \rangle^2 + L_3 \langle D_\mu U D^\mu U^\dagger D_\nu U D^\nu U^\dagger \rangle \\ & + L_4 \langle D_\mu U D^\mu U^\dagger \rangle \langle \chi U^\dagger + U \chi^\dagger \rangle + L_5 \langle (D_\mu U D^\mu U^\dagger) (\chi U^\dagger + U \chi^\dagger) \rangle \\ & + L_6 \langle \chi U^\dagger + U \chi^\dagger \rangle^2 + L_7 \langle \chi U^\dagger - U \chi^\dagger \rangle^2 + L_8 \langle \chi U^\dagger \chi U^\dagger + \chi^\dagger U \chi^\dagger U \rangle \\ & + i L_9 \langle L_{\mu\nu} D^\mu U D^\nu U^\dagger + R_{\mu\nu} D^\mu U^\dagger D^\nu U \rangle + L_{10} \langle L_{\mu\nu} U R^{\mu\nu} U^\dagger \rangle \end{aligned} \quad (39)$$

where L_i are the expansion coefficients that must be determined phenomenologically. Both \mathcal{L}_2 and \mathcal{L}_4 are invariant under

$$U \leftrightarrow U^\dagger, \quad \chi \leftrightarrow \chi^\dagger, \quad \ell_\mu \leftrightarrow r_\mu \quad (40)$$

since the trace is invariant under cyclic shifting of matrices. This is the so-called intrinsic parity operation (originally introduced by Witten [2]), which operates on the function, but not on the space-time coordinates. If $\ell_\mu = r_\mu$, then we can have terms containing an odd or even number of pseudoscalars, but no transition between the two, as this would violate intrinsic parity conservation. ℓ_μ is equal to r_μ if we have only EM interactions or direct meson interaction (no external fields). Including the W fields, the two sectors of differing intrinsic parity are coupled and intrinsic parity can be violated. Hence, both \mathcal{L}_2 and \mathcal{L}_4 are unable to describe anomalous processes like $3\pi 2K$ or $\pi^0 \gamma \gamma$. For further details see [3].

What have we missed? There is the possibility of terms that transform non-trivially under G , but still preserve chiral symmetry if their variation under G is a total derivative [2]. This type of term is anomalous.

In order to describe anomalous processes we need terms that take the axial anomaly into account. The first terms that contribute are $\mathcal{O}(p^4)$ and make up the so-called Wess-Zumino-Witten anomalous action.

4.5 Anomalous Processes

In this thesis we consider a number of anomalous processes. First we have the pseudoscalar to $\gamma\gamma^*$ decays: $\pi^0/\eta \rightarrow \gamma\gamma^*$, where γ^* is on-shell or off-shell going to an e^+e^- pair. We also

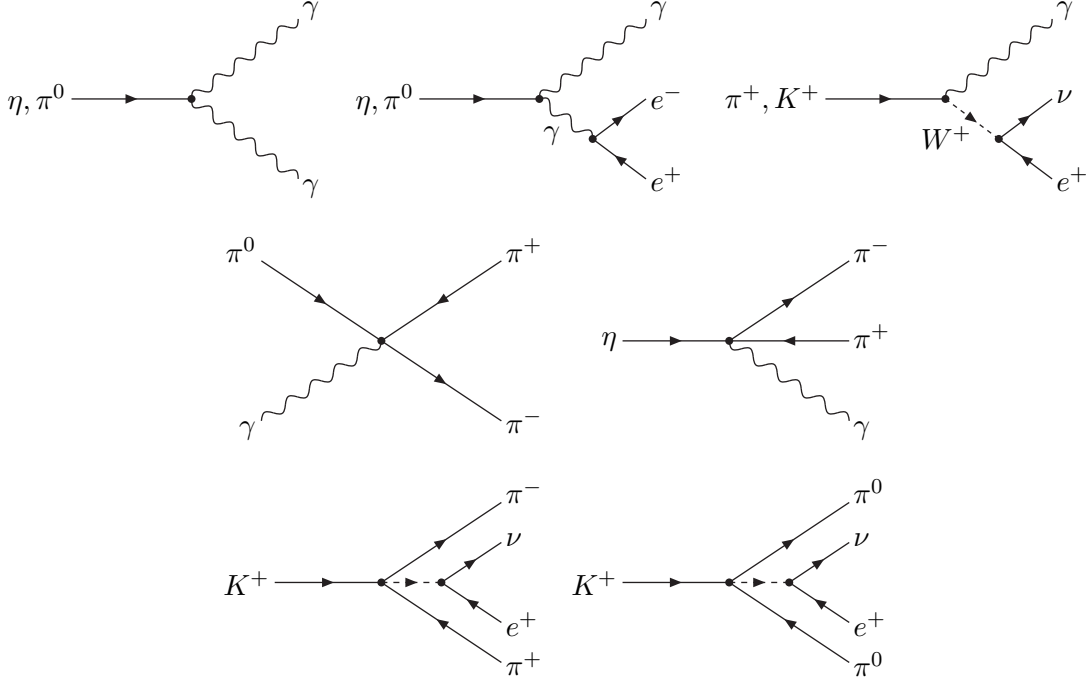


Figure 1: *Feynman diagrams for the anomalous processes.*

consider the semileptonic weak decays $\pi^+/K^+ \rightarrow \gamma e^+ \nu_e$, $K^+ \rightarrow \pi^+ \pi^- e^+ \nu$, $K^+ \rightarrow \pi^0 \pi^0 e^+ \nu$ and the three-pseudoscalar-photon interactions $\gamma \pi^- \rightarrow \pi^- \pi^0$ and $\eta \rightarrow \pi^+ \pi^- \gamma$. The η calculations were performed for both the octet η_8 and the singlet η_0 component, but only the octet is relevant at the level we're working at. The Feynman diagrams for the processes are depicted in figure 1.

5 $\eta'(958)$

Invoking the quark model, we see that the quantum numbers of $\pi^+, \pi^-, \pi^0, K^+, K^-, K^0, \bar{K}^0$ and η_8 are the same as for $u\bar{d}, d\bar{u}, (u\bar{u} - d\bar{d}), u\bar{s}, s\bar{u}, d\bar{s}, s\bar{d}$ and $(u\bar{u} + d\bar{d} - 2s\bar{s})$. Extending this logic, we find one more state $u\bar{u} + d\bar{d} + s\bar{s}$, identifiable with the next lightest pseudoscalar meson in turn, the $\eta'(958)$. The η' has an abnormally large mass compared to the other pseudoscalars. This is because it receives a mass contribution from the axial $U(1)_A$ anomaly [9]. By Noether's theorem the axial $SU(3)$ singlet current is $J_{5\mu}^{(0)} = \sum_{q=u,d,s} \bar{q} \gamma_5 q$, the divergence of which receives an anomalous contribution

$$\partial^\mu J_{5\mu}^{(0)} = \frac{3\alpha_s}{8\pi} G_{\mu\nu}^a \tilde{G}^{a\mu\nu} + 2im_q \sum_{q=u,d,s} \bar{q} \gamma_5 q \quad ; \quad \tilde{G}^{a\mu\nu} \equiv \varepsilon^{\mu\nu\alpha\beta} G_{\alpha\beta}^a \quad (41)$$

where $G_{\mu\nu}$ is the field strength tensor for the strong interaction and $\varepsilon^{\mu\nu\alpha\beta}$ the antisymmetric Levi-Civita tensor. Taking the divergence of the vacuum to η_0 matrix element, we get

$$\langle 0 | J_{5\mu}^{(0)} | \eta_0(\mathbf{p}) \rangle = iF_{\eta_0} p_\mu e^{-ip \cdot x} \Rightarrow \quad (42)$$

$$\langle 0 | \partial^\mu J_{5\mu}^{(0)} | \eta_0(\mathbf{p}) \rangle = F_{\eta_0} m_{\eta_0}^2 \Rightarrow \quad (43)$$

$$\lim_{m_q \rightarrow 0} m_{\eta_0}^2 = \frac{1}{F_{\eta_0}} \frac{3\alpha_s}{8\pi} \langle 0 | G_{\mu\nu}^a \tilde{G}^{a\mu\nu} | \eta_0(\vec{p}) \rangle \quad (44)$$

which tells us that the η_0 mass is non-vanishing in the chiral limit. If it were not for the anomalous $G\tilde{G}$ -term the $U(1)_A$ symmetry would be approximately conserved and break dynamically along with the chiral $SU(3)$, producing a nonet of GS bosons.

6 $\eta_8 - \eta_0$ mixing

$SU(3)$ breaking in the quark mass matrix causes the singlet η_0 and octet η_8 components to mix, yielding the physical states η and η' .

$$\begin{pmatrix} |\eta\rangle \\ |\eta'\rangle \end{pmatrix} = \begin{pmatrix} \cos\theta & -\sin\theta \\ \sin\theta & \cos\theta \end{pmatrix} \begin{pmatrix} |\eta_8\rangle \\ |\eta_0\rangle \end{pmatrix} ; \begin{cases} |\eta_8\rangle = \frac{1}{\sqrt{6}}(u\bar{u} + d\bar{d} - 2s\bar{s}) \\ |\eta_0\rangle = \frac{1}{\sqrt{3}}(u\bar{u} + d\bar{d} + s\bar{s}) \end{cases} \quad (45)$$

Quantum mechanically, other states with $I = 0$ can also enter the mix. These we assume to be too heavy to be of significance. Another crucial assumption is that the mixing does not depend on the energy of the state, which allows for this simple phenomenologically motivated model [12]. Making use of the π^0, η, η' to $\gamma\gamma$ data, the mixing angle θ is determined to be approximately -20° . With this angle we find the quark content

$$\eta \sim 0.58(u\bar{u} + d\bar{d}) - 0.57s\bar{s} \quad (46)$$

$$\eta' \sim 0.40(u\bar{u} + d\bar{d}) + 0.82s\bar{s} \quad (47)$$

The $s\bar{s}$ is decreased for the η , and increased for the η' , accounting for the large mass difference. Since the up quark has a greater charge magnitude, the $\eta \rightarrow \gamma\gamma$ amplitude is boosted. Heuristically, this can be seen by

$$\begin{aligned} A &\sim e_u^2 \left(\frac{\cos\theta}{\sqrt{6}} - \frac{\sin\theta}{\sqrt{3}} \right) + e_d^2 \left(\frac{\cos\theta}{\sqrt{6}} - \frac{\sin\theta}{\sqrt{3}} \right) + e_s^2 \left(-\frac{2\cos\theta}{\sqrt{6}} - \frac{\sin\theta}{\sqrt{3}} \right) \\ &\propto \begin{cases} \frac{1}{\sqrt{6}} & ; \theta = 0 \\ \frac{1}{\sqrt{3}} & ; \theta \simeq 20^\circ \end{cases} \end{aligned} \quad (48)$$

so that there is a factor 2 difference in width if we take the mixing into account. This mixing model can also be directly encoded into the chiral coefficients, but offers an explanation for lowest order experimental-theoretical discrepancies.

7 Anomalies

Anomalies are said to appear whenever a classical symmetry is violated by the existence of quantum corrections. They are crucial in expanding the theoretical framework, as they signal new physics in the standard model. In this section we examine the origin of the anomaly.

7.1 Classical vs. Quantum Symmetries

Let's compare the classical Noether current with the one obtained from the full quantum theory using path integrals. A more complete treatment of the subject can be found in [9]. The infinitesimal transformation

$$\varphi_i \rightarrow \varphi'_i = \varphi_i + \varepsilon(x) f_i(\varphi), \quad (49)$$

where $\varepsilon(x)$ is the infinitesimal parameter (which is temporarily given a coordinate dependence for the purposes of Noether current construction) and f_i is an arbitrary function of the fields, implies a Noether current and an invariance condition:

$$J^\mu(x) = \frac{\partial \mathcal{L}'}{\partial (\partial_\mu \varepsilon)} \Rightarrow \mathcal{L}(\varphi', \partial \varphi') = \mathcal{L}(\varphi, \partial \varphi) + J^\mu \partial_\mu \varepsilon \quad (50)$$

So that the Lagrangian is invariant if ε is a constant. (50) represents the classical symmetry.

In the path integral formalism, all matrix elements can be obtained via the generating functional $W[j]$, which is a functional of the sources.

$$W[j] = e^{iZ[j]} = \int [d\varphi] e^{i \int d^4x (\mathcal{L}(\varphi, \partial \varphi) - j\varphi)} \quad (51)$$

where the classical source field $j(x)$ is used to probe the theory, and where $[d\varphi]$ stands for integration over all possible values of $\varphi(x)$ at each space-time point. Matrix elements describing physical processes are obtained by taking the functional derivative² of the logarithm of the path integral.

$$\langle 0 | T(\varphi(x_k) \dots \varphi(x_p)) | 0 \rangle = (i)^n \frac{\delta^n \ln W[j]}{\delta j(x_k) \dots \delta j(x_p)} \quad (52)$$

We can study the classical Noether current $J^\mu(x)$ by coupling it to a classical source field v_μ and inserting it in the generating functional (51).

$$W[v_\mu] = \int [d\varphi] e^{i \int d^4x (\mathcal{L}(\varphi, \partial \varphi) - v_\mu J^\mu)} \quad (53)$$

(52) lets us take current matrix elements (denoted by bar),

$$\bar{J}^\mu(x) = i \frac{\delta \ln W[v_\nu]}{\delta v_\mu(x)} \Rightarrow \quad (54)$$

$$\delta \ln W[v_\mu] = \ln W[v_\mu + \delta v_\mu] - \ln W[v_\mu] \equiv -i \int d^4x \bar{J}^\mu(x) \delta v_\mu(x) \quad (55)$$

If we choose $\delta v_\mu = -\partial_\mu \varepsilon(x)$, then

$$\delta_\varepsilon \ln W[v_\mu] = \ln W[v_\mu - \partial_\mu \varepsilon] - \ln W[v_\mu] \quad (56)$$

$$= i \int d^4x \bar{J}^\mu(x) \partial_\mu \varepsilon(x) = -i \int d^4x \varepsilon(x) \partial_\mu \bar{J}^\mu(x) \quad (57)$$

²Functional differentiation is defined by

$$j(t) = \int dt' \delta(t - t') j(t') \Rightarrow \frac{\delta j(t)}{\delta j(t')} = \delta(t - t')$$

where in the last step partial integration has been used. From this follows that if $\delta_\varepsilon \ln W[v_\mu] = 0$ then all matrix elements are divergenceless, i.e. $\partial^\mu \bar{J}_\mu(x) = 0$.

Since we are integrating over all values of $\varphi(x)$ at each point in space-time, one can argue that it should make no difference if we shift the origin of integration at each point x by a constant, redefining $\varphi_i(x) \equiv \varphi'_i(x) - \varepsilon(x) f_i(\varphi)$, as in (49), with an accompanying Jacobian $\mathcal{J} = 1$.

$$\ln W[v_\mu - \partial_\mu \varepsilon] = \int [d\varphi_i] e^{i \int d^4x (\mathcal{L}(\varphi, \partial\varphi) - (v_\mu - \partial_\mu \varepsilon) J^\mu)} \quad (58)$$

$$= \int [d\varphi'_i] e^{i \int d^4x (\mathcal{L}(\varphi', \partial\varphi') - v_\mu J^\mu)} = \ln W[v_\mu] \quad (59)$$

This would imply $\partial^\mu \bar{J}_\mu(x) = 0$, in accordance with classical current conservation. However, as was first shown by Fujikawa [13], shifting the origin like this is not always allowed. The transformation (49) can have a Jacobian $\mathcal{J} \neq 1$, so that the path integral measure is changed. If the change of variables is non-trivial then $\partial^\mu \bar{J}_\mu(x) \neq 0$, and we have encountered an anomaly.

7.2 The $U(1)_A$ Axial Anomaly

In the chiral limit, the QCD Lagrangian is invariant under the global $U(1)_A$ axial transformation $\psi \rightarrow e^{-i\theta\gamma_5} \psi$. Using Noether's theorem we get the classically conserved singlet current $J_{5\mu}^{(0)} = \sum \bar{q} \gamma_\mu \gamma_5 q$, with $\partial^\mu J_{5\mu}^{(0)} = 0$. However, in going through the full quantum theory analysis, it is found that the divergence of the matrix elements of the axial vector singlet current is proportional an anomaly,

$$\partial^\mu J_{5\mu}^{(0)} = \frac{3\alpha_s}{8\pi} G_{\mu\nu}^a \tilde{G}^{a\mu\nu} \quad ; \quad \tilde{G}_{\mu\nu}^a \equiv \varepsilon^{\mu\nu\alpha\beta} G_{\alpha\beta}^a \quad (60)$$

Important consequences of the anomaly involves a large anomalous contribution to the $\pi^0 \rightarrow \gamma\gamma$ decay rate, the prevention of η' becoming a Goldstone boson (thus separating the chiral $SU(3)$ spectra into one octet and one singlet part).

There are two main approaches one can take in examining the anomaly: 1) a direct calculation via the $U(1)_A \rightarrow gg$ triangle diagram, or 2) the path integral analysis. The direct approach was originally taken by the discoverers of the $U(1)_A$ anomaly³: Adler [14], Bell and Jackiw [15]. They calculated the matrix element for the $U(1)_A$ current going to two gluons via the Feynman diagram in figure 2. In the resulting four-momentum integral we can make a change of variables, yielding an expression that is compatible with conservation of the vector color current or the $U(1)_A$ current, but not both. Phenomenologically, we know that only the vector color current is conserved. In the presence of the $U(1)_A$ anomaly, the axial symmetry is not even approximately conserved. The anomaly is also present in the $U(1)_A \rightarrow \gamma\gamma$ diagram, producing equation (60) with $\alpha_s \rightarrow \alpha_{EM}$ and $G_{\mu\nu} \rightarrow F_{\mu\nu}$.

The path integral approach was taken by Fujikawa [13], and clarifies the origin of the anomaly. In the path integral formalism we introduce the singlet axial current coupled to an axial current source a_μ into a functional of the gluon field A_μ^a .

$$W[a_\mu, A_\mu^a] = \int [d\bar{\psi}][d\psi] e^{i \int d^4x (\mathcal{L}_{QCD}(\psi, \bar{\psi}, A_\lambda^a) - a_\mu J_5^{(0)\mu})} \quad (61)$$

³A.k.a. the Adler-Bell-Jackiw anomaly.

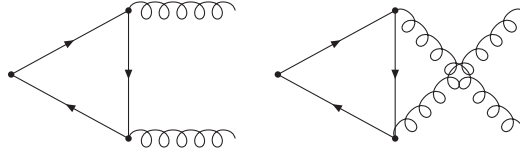


Figure 2: $U(1)_A \rightarrow gg$ diagrams leading to an axial vector anomaly.

The crucial point is that in redefining the fermion fields to absorb the ε term of eq. (59), the path integral measure is changed:

$$\int [d\bar{\psi}][d\psi] = \mathcal{J} \int [d\bar{\psi}'][d\psi'] \quad (62)$$

where the Jacobian \mathcal{J} is independent of the fermion fields. The Jacobian is divergent, but can be regularized (as was done by Fujikawa) by removing the high energy eigenmodes of the Dirac field in a gauge invariant way. The freedom to change integration variables in the direct approach, corresponds to the freedom in choice of regulator in the path integral approach.

8 The Wess-Zumino-Witten (WZW) Anomaly Action

In section 4.4 we saw that if we want to describe anomalous processes, we must construct an effective Lagrangian that violates intrinsic parity. This can be ensured by always including the totally antisymmetric Levi-Civita tensor $\varepsilon^{\mu\nu\alpha\beta}$, the presence of which will preserve normal parity while at the same time violating intrinsic parity. The origin of this symmetry breaking lies in the axial anomaly. It affects photonic processes like $\pi^0 \rightarrow \gamma\gamma$, but also hadronic ones like $K\bar{K} \rightarrow \pi^0\pi^+\pi^-$. For reactions like these we need to construct a Lagrangian, which takes the axial anomaly into account. This section contains a brief sketch of how this can be done. The derivation follows the sigma model approach employed by Donoghue et al [9].

The history of the anomalous $\mathcal{O}(p^4)$ WZW action follows a somewhat crooked path. The first effective action analysis of the anomaly was made by Wess and Zumino, who arrived at their expression by integrating the anomalous Ward identities [1]. Their Lagrangian was given as a Taylor expansion, and was later given a geometric interpretation and rewritten on a compact form as a five-dimensional integral with four-dimensional space-time boundaries by Witten [2] (his form did not conserve parity, but was later corrected).

8.1 Anomalous Terms

We emulate QCD behavior by introducing a color quantum number (with N_c colors), and we are using the u, d, s quarks so the number of fermions is set to three (all with mass M). All that is needed to derive the anomalous action are the correct symmetries. A convenient starting point is the sigma model, which incorporates the essential features of spontaneous symmetry breaking and chiral invariance. Making use of the representation independence theorem one can then proceed with the non-linear sigma model using exponential parametrization. This facilitates the extension of the formalism from 2 to 3 flavors. Dropping all terms irrelevant

to the anomaly and imposing the unitary change of variables $\psi_L \rightarrow \xi^\dagger \psi_L$, $\psi_R \rightarrow \xi \psi_R$, one arrives at a Lagrangian for fermions of mass M coupled to axial and vector sources.

$$\mathcal{L} = \bar{\psi} (i\mathcal{P} - M) \psi \quad (63)$$

where

$$D_\mu = \partial_\mu + i\bar{V}_\mu + i\bar{A}_\mu \gamma_5 \quad ; \quad \bar{V}_\mu = -\frac{i}{2} \left(\xi^\dagger \partial_\mu \xi + \xi \partial_\mu \xi^\dagger \right) \quad (64)$$

$$; \quad \bar{A}_\mu = -\frac{i}{2} \left(\xi^\dagger \partial_\mu \xi - \xi \partial_\mu \xi^\dagger \right) \quad (65)$$

Our model contains no gluons, but according to the Adler-Bardeen theorem [16] this will not modify the result. Keeping in mind the section on anomalies, we see that the change of variables induces a change in the path integral measure, and the Jacobian must enter into the effective action.

$$e^{i\Gamma(U)} = \int [d\psi] [d\bar{\psi}] \mathcal{J} e^{i \int d^4x \bar{\psi} (i\mathcal{P} - M) \psi} = e^{\ln \mathcal{J}} e^{\text{tr} \ln (i\mathcal{P} - M)} \quad (66)$$

The second exponent cannot produce $\varepsilon^{\mu\nu\alpha\beta}$ at $\mathcal{O}(p^4)$, so the anomalous effect must be lodged in the Jacobian. Having the distinct goal of calculating the Jacobian in mind, we introduce a continuous parameter dependence via the transformation $\xi \rightarrow \xi_\tau = \exp(i\tau \vec{\lambda} \cdot \vec{\varphi}/2F_\pi) \equiv \exp(i\tau \vec{\varphi})$. Transforming infinitesimally in τ induces a change $\delta\mathcal{J}$ in the Jacobian,

$$\psi \rightarrow \psi' = \xi_{\delta\tau}^\dagger \psi_L + \xi_{\delta\tau} \psi_R \Rightarrow \int [d\psi] [d\bar{\psi}] = \int [d\psi'] [d\bar{\psi}'] e^{\ln \delta\mathcal{J}} \quad (67)$$

$$\Rightarrow \delta\mathcal{J} = e^{-2i\delta\tau \text{tr} \bar{\varphi} \gamma_5} \Rightarrow \left. \frac{d \ln \mathcal{J}}{d\tau} \right|_{\tau=0} = -2i \text{tr} \bar{\varphi} \gamma_5 \quad (68)$$

Due to the anomaly, the Jacobian is divergent and must be regularized. Making use of Fujikawas method of removing high energy eigenmodes in a gauge invariant way we take the limit

$$\text{tr} \bar{\varphi} \gamma_5 = \lim_{\varepsilon \rightarrow 0} \text{tr} \left(\bar{\varphi} \gamma_5 e^{-\varepsilon \mathcal{P}_\tau \mathcal{P}_\tau} \right) \quad ; \quad \mathcal{P}_\tau \equiv \partial^\mu + i\bar{V}_\tau^\mu + i\bar{A}_\tau^\mu \gamma_5 \quad (69)$$

From the definition of vector and axial-vector currents (64) with $\xi \rightarrow \xi_\tau$, we have that

$$\begin{aligned} \mathcal{P}_\tau \mathcal{P}_\tau &= d_\mu d^\mu + \sigma \quad ; \quad d_\mu = \partial_\mu + i\bar{V}_{\tau\mu} + \sigma_{\mu\nu} \bar{A}_\tau^\nu \gamma_5 = \partial_\mu + \Gamma_{\tau\mu} \\ &\quad ; \quad \sigma = -2\bar{A}_{\tau\mu} \bar{A}_\tau^\mu + i [\partial_\mu + i\bar{V}_{\tau\mu}, \bar{A}_\tau^\mu] \gamma_5 \end{aligned} \quad (70)$$

We now make use of the heat kernel expansion from thermodynamics and take the limit $\varepsilon \rightarrow 0$, to obtain an expression for the regulated anomalous action $\Gamma(\bar{\varphi})$.

$$\text{tr} \bar{\varphi} \gamma_5 = i \int d^4x \text{Tr} \left(\frac{\bar{\varphi} \gamma_5}{(4\pi\varepsilon)^2} \sum_n \varepsilon^n a_n \right) \xrightarrow{\varepsilon \rightarrow 0} \frac{i}{16\pi^2} \int d^4x \text{Tr} (\bar{\varphi} \gamma_5 a_2) \Rightarrow \quad (71)$$

$$\Gamma(\bar{\varphi}) = -i \ln \mathcal{J} + \dots = \frac{N_c}{4\pi^2} \int_0^1 d\tau \int d^4x \text{Tr} \left(\frac{8}{3} \bar{\varphi} \varepsilon_{\mu\nu\alpha\beta} \bar{A}_\tau^\mu \bar{A}_\tau^\nu \bar{A}_\tau^\alpha \bar{A}_\tau^\beta \right) + \dots \quad (72)$$

where N_c comes from the color sum and the ellipses signify terms without correct symmetry ($\varepsilon_{\mu\nu\alpha\beta}$). The only way to integrate this expression in a closed form, is to Taylor expand each axial-vector current around $\tau = 0$, and then integrate to obtain a series of local Lagrangians.

What Witten did was to treat the τ as a time-like fifth dimension x_5 , with $\tau = 1$ corresponding to normal space-time. By expansion one can prove that the final result depends only on normal space-time. To describe processes other than direct meson interaction, we must include external electroweak gauge fields via ℓ_μ and r_μ . This will alter the covariant derivative, which in turn affects the Jacobian. The result is a gauge invariant tree-level action describing the effect of the anomaly at $\mathcal{O}(p^4)$ in the chiral expansion.

The WZW action can be written on a form more suitable for calculations, by performing the τ integration where possible and changing variables [6].

$$S[U, \ell, r]_{WZW} = -\frac{iN_c}{240\pi^2} \int d\sigma^{ijklm} \langle \Sigma_i^L \Sigma_j^L \Sigma_k^L \Sigma_l^L \Sigma_m^L \rangle - \frac{iN_c}{48\pi^2} \int d^4x \varepsilon_{\mu\nu\alpha\beta} \left(W(U, \ell, r)^{\mu\nu\alpha\beta} - W(\mathbf{1}, \ell, r) \right) \quad (73)$$

where

$$\begin{aligned} W(U, \ell, r)_{\mu\nu\alpha\beta} = & \langle U \ell_\mu \ell_\nu \ell_\alpha U^\dagger r_\beta + \frac{1}{4} U \ell_\mu U^\dagger r_\nu U \ell_\alpha U^\dagger r_\beta \\ & + i U \partial_\mu \ell_\nu \ell_\alpha U^\dagger r_\beta + i \partial_\mu r_\nu U \ell_\alpha U^\dagger r_\beta - i \Sigma_\mu^L \ell_\nu U^\dagger r_\alpha U \ell_\beta \\ & + \Sigma_\mu^L U^\dagger \partial_\nu r_\alpha U \ell_\beta - \Sigma_\mu^L \Sigma_\nu^L U^\dagger r_\alpha U \ell_\beta + \Sigma_\mu^L \ell_\nu \partial_\alpha \ell_\beta + \Sigma_\mu^L \partial_\nu \ell_\alpha \ell_\beta \\ & - i \Sigma_\mu^L \ell_\nu \ell_\alpha \ell_\beta + \frac{1}{2} \Sigma_\mu^L \ell_\nu \Sigma_\alpha^L \ell_\beta - i \Sigma_\mu^L \Sigma_\nu^L \Sigma_\alpha^L \ell_\beta \rangle - (L \leftrightarrow R) \end{aligned} \quad (74)$$

where

$$\begin{cases} \Sigma_\mu^L = U^\dagger \partial_\mu U \\ \Sigma_\nu^R = U \partial_\mu U^\dagger \end{cases} \quad (75)$$

and

$$U = \exp \left[i \frac{\sqrt{2}}{F} \begin{pmatrix} \frac{\pi^0}{\sqrt{2}} + \frac{\eta}{\sqrt{6}} & \pi^+ & K^+ \\ \pi^- & -\frac{\pi^0}{\sqrt{2}} + \frac{\eta}{\sqrt{6}} & K^0 \\ K^- & \bar{K}^0 & -\frac{2}{\sqrt{6}}\eta \end{pmatrix} \right] \quad (76)$$

$L \leftrightarrow R$ stands for

$$\begin{cases} U \leftrightarrow U^\dagger \\ \ell_\mu \leftrightarrow r_\mu \\ \Sigma_\mu^L \leftrightarrow \Sigma_\mu^R \end{cases} \quad (77)$$

8.2 Example of Calculation

As an example of how to use (73) we calculate the amplitude for $\pi^0 \rightarrow \gamma e^+ e^-$. The five dimensional term does not contribute as it contains too many fields. The second term in the normal space-time integral is just there for mathematical consistency, which leaves us with $W_{\mu\nu\alpha\beta}$. It's easy to see that the $L \leftrightarrow R$ operation leads to the same result (since $\ell_\mu = r_\mu$). So we can calculate just the L terms and then multiply by 2. Below we have used partial integration and the antisymmetry of $\varepsilon^{\mu\nu\alpha\beta}$.

$$\begin{aligned}
W_{\mu\nu\alpha\beta} &= 2 \left\langle \Sigma_\mu^L U^\dagger \partial_\nu r_\alpha U \ell_\beta + \Sigma_\mu^L \ell_\nu \partial_\alpha \ell_\beta + \Sigma_\mu^L \partial_\nu \ell_\alpha \ell_\beta \right\rangle \\
&= i \frac{2\sqrt{2}}{F} e^2 \langle \partial_\mu M \partial_\nu A_\alpha A_\beta Q^2 + \partial_\mu M A_\nu \partial_\alpha A_\beta Q^2 + \partial_\mu M \partial_\nu A_\alpha A_\beta Q^2 \rangle \\
&= -i \frac{e^2}{F} 6\sqrt{2} \langle M Q^2 \rangle \partial_\mu A_\nu \partial_\alpha A_\beta = -i 2 \frac{e^2}{F} \partial_\mu A_\nu \partial_\alpha A_\beta \Rightarrow \\
A(\pi^0 \rightarrow \gamma\gamma^*) &= i \frac{1}{4\pi^2} \frac{e}{F} \varepsilon^{\mu\nu\alpha\beta} k_\mu \varepsilon_\nu k_\alpha^* \varepsilon_\beta^* \tag{78}
\end{aligned}$$

where the $\pi^0 \rightarrow \gamma e^+ e^-$ amplitude can easily be obtained by applying the Feynman rules for QED. ε is the photon polarization vector and k the photon 4-momentum. The $\pi^0 \rightarrow \gamma\gamma$ decay is historically important as it paved the way for the theory of the anomalous sector. This is where Steinberger [17] in 1949 first observed the effects of the anomaly.

In contrast with the effective Lagrangians, the only parameter appearing in the WZW action is N_c ⁴. This is because it is a prediction of the QCD anomaly structure. In accordance with Adler and Bardeen [16] there are no radiative corrections. One can show that N_c is an integer by making use of the fact that the five-dimensional integral can only depend on normal four-dimensional space-time.

Squaring the matrix element, summing over photon polarizations and inserting one half for identical particles gives

$$\begin{aligned}
|A_{WZW}^{\pi^0\gamma\gamma}|^2 &= \frac{N_c^2 \alpha^2}{9\pi^2 F_\pi^2} \frac{1}{2} \sum_{Pol} \varepsilon^{\mu\nu\alpha\beta} \varepsilon_\mu k_\nu \varepsilon_\alpha^* k_\beta^* \varepsilon_{\mu'\nu'\alpha'\beta'} \varepsilon^{\mu'} k^{\nu'} \varepsilon^{\alpha'*} k^{\beta'*} \quad ; \begin{cases} \varepsilon/\varepsilon^* = (0, 1, 0, 0) \\ \varepsilon^*/\varepsilon = (0, 0, 1, 0) \\ k/k^* = \frac{m_\pi}{2} (1, 0, 0, \pm 1) \end{cases} \\
\sum_{Pol} \dots &= -2 \times (2013) (2310) - 2 \times (1023) (1320) \quad ; (2013) = \varepsilon_2 k_0 \varepsilon_1^* k_3^* \text{ etc.} \\
&+ (2013)^2 + (2310)^2 + (1023)^2 + (1320)^2 = \frac{1}{2} m_\pi^4 \Rightarrow \\
\Gamma_{\gamma\gamma} &= \frac{1}{16\pi} \frac{|A_{WZW}|^2}{m_\pi} = \frac{1}{16\pi m_\pi} \frac{N_c^2 \alpha^2}{9\pi^2 F_\pi^2} \frac{1}{2} \frac{1}{2} m_\pi^4 \xrightarrow{N_c=3} \frac{\alpha^2}{64\pi^3 F_\pi^2} m_\pi^3 \simeq 7.73 \text{ eV}
\end{aligned}$$

In excellent agreement with the experimental value $\Gamma_{\gamma\gamma} = 7.7 \pm 0.5 \pm 0.5 \text{ eV}$ [18]. This is an important test for the number of colors as well as the anomaly structure and chiral symmetries.

In section 10 we follow through with the $\mathcal{O}(p^6)$ contribution to $\pi^0 \rightarrow \gamma\gamma^*$, allowing us to solve for the chiral coefficients.

9 Loops and Renormalization

The anomalous sector is subject to meson loop corrections. QFT loop corrections to the Born amplitude lead to ultra-violet divergences in the form of polynomials in masses or external momenta. All non-analytical divergences must cancel. The UV divergences are removed by introducing a finite number of counterterms at a given order. Poles from one loops in dimensional regularization can be obtained by considering quantum fluctuations around the classical solution of the EOM.

⁴One can also introduce the number of fermions N_f , which we here set to 3.

9.1 Power Counting

In this section we consider the order at which a general Feynman diagram contributes. The distinction should be clear from section 4.2 where we are asking which tree-level terms will contribute at a given order. Here we follow a purely diagrammatic approach (as in [9]) to arrive at Weinberg's power counting theorem [19]. We are specifically interested in the order at which loop integrals contribute.

Consider a general diagram with N_V vertices and N_n vertices from \mathcal{L}_n , so that $N_V = \sum_n N_n$. The dimensionality of the couplings is M^{N_C} , where $N_C = \sum_n N_n (4 - n)$ and M is the characteristic mass scale. For N_I internal lines and N_E external lines we get $M^{2N_I - N_E}$. There is a relation between internal lines, vertices and loops;

$$N_I = N_L + N_V - 1 = N_L + \sum_n N_n - 1 \quad (79)$$

Remaining factors must be composed of a power of energy times the logarithm of the dimensionless E^2/μ^2 (where μ is the renormalization scale). Putting all this together, we get the matrix element energy dimensionality

$$\mathcal{M} \sim \frac{M^{\sum_n N_n (4-n)}}{M^{N_E + 2N_L + 2\sum_n N_n - 2}} E^D F(E/\mu) \Rightarrow D = 2 + \sum_n N_n (n - 2) + 2N_L \quad (80)$$

So that a diagram with N_L loops contributes at E^{2N_L} higher than the tree-level used in the calculation. This simplifies calculations considerably, since at low energies, only a few loops need to be taken into account. Loop divergences are handled in the usual way, and can be removed by renormalizing the parameters of the theory. The general effective Lagrangian, compatible with the symmetry conditions, must have enough parameters to absorb the divergences.

The lowest order action for anomalous processes is already $\mathcal{O}(p^4)$ (the WZW action). At $\mathcal{O}(p^4)$ we have the power counting: tree level diagrams from S_{WZW} with one vertex, and the rest from \mathcal{L}_2 . In this thesis we will proceed up to the $\mathcal{O}(p^6)$ anomalous action. At $\mathcal{O}(p^6)$ we have: tree level diagrams with one vertex from S_{WZW} , one from \mathcal{L}_4 and the rest from \mathcal{L}_2 , tree level diagrams with one vertex from the anomalous $\mathcal{O}(p^6)$ action and the rest from \mathcal{L}_2 , one-loop diagrams with one vertex from S_{WZW} and the rest from \mathcal{L}_2 .

9.2 Infinite parts

Starting from a chiral-invariant effective Lagrangian, the divergences from the loop integrals are constrained by chiral symmetry. In the previous section we saw that one-loops contribute at $\mathcal{O}(p^2)$ higher than the order of the Lagrangian from which they were calculated. The anomalous power counting laws tell us that chiral invariant counterterms in the anomalous Lagrangian of $\mathcal{O}(p^6)$ will absorb the one-loop divergences, leaving behind the renormalized coefficients. To calculate the divergent parts of the \mathcal{L}_2 one-loops, we can expand around the classical solution to the EOMs of our chiral theory, i.e. the GS boson matrix.

$$\begin{aligned} \frac{\delta S_2}{\delta U} &= 0 \Rightarrow \bar{U} = e^{i \frac{\sqrt{2}}{F_\pi} M} \\ U &= e^{i \frac{\sqrt{2}}{F} (M + \xi')} = e^{i \frac{M}{\sqrt{2}F}} e^{i \xi} e^{i \frac{M}{\sqrt{2}F}} = u e^{i \xi} u \end{aligned}$$

where ξ is an Hermitian matrix that preserves unitarity. The one-loop divergences are obtained by expanding \mathcal{L}_2 (eq. (29)) to $\mathcal{O}(\xi^2)$:

$$\int d^4x \mathcal{L}_2 = \int d^4x \bar{\mathcal{L}}_2 + \frac{1}{2} \int d^4x \xi^i \Delta_{ij} \xi^j + \mathcal{O}(\xi^3) \quad (81)$$

The divergent parts of the new term in (81) can be pinpointed by calculating the second variation of S_2 and identifying the relevant operators. The power counting of section 9.1 told us that the WZW action can contribute a vertex to one-loop diagrams. Including the WZW action, the equations of motion and the variation of second order in ξ now receives new contributions, and the corresponding anomalous quantities are calculated through the second variation of S_{WZ} . The calculation of divergent terms is very technical and the reader is referred to [3] for a more in-depth analysis.

9.3 Meson One-Loop Corrections

We begin by considering the $PS \rightarrow \gamma\gamma^*$ decays. If both photons are on-shell there are no infinite parts coming from the meson one-loops. This means that we should find no counterterms in the chiral coefficients describing the decay. If however, the photon goes to an e^+e^- pair, coefficients containing parts designated to cancel the infinities will appear. The meson one-loop corrections were calculated by Bijmens et al. [20] via the Feynman diagrams in figure 3. To fully describe situation we must include the results from the wavefunction renormalization and the decay constant corrections. For the semileptonic $\pi^+/K^+ \rightarrow \gamma e^+\nu$ decays, the one-loops corrections have been calculated in [21]. These have Feynman diagrams similar to those in figure 3.

We are also considering the experimentally well charted 3-pseudoscalar-photon interactions $\eta\pi\pi\gamma$ & $\pi\pi\pi\gamma$. The one-loop corrections were calculated in [27] via the Feynman diagrams in figure 4. Only on-shell photons are considered here. For $\pi\pi\pi\gamma$, k_γ^2 is very small ($\ll m_\pi^2$), and for $\eta\pi\pi\gamma$ $k_\gamma^2 = 0$ unless $e^+e^- \rightarrow \gamma^* \rightarrow 3\pi$, which we do not consider. The decays $K^+ \rightarrow \pi^+\pi^-e^+\nu$ and $K^0 \rightarrow \pi^0\pi^-e^+\nu$ are subject to similar loop corrections (as calculated in [21]).

In the loop corrections (listed in appendix A) we find the so-called chiral logarithms of the form $m_{PS}^2 \log m_{PS}^2/\mu^2$, where $\mu = m_\rho$ is taken as the arbitrary renormalization scale. We also find the divergent terms proportional to λ (see eq. (83)), which will be exactly canceled by the counterterms at $\mathcal{O}(p^6)$. These are either proportional to pseudoscalar masses or particle four-momenta. The latter can be seen to vanish in the soft (low energy) limit. Most loop corrections were calculated using $m_u = m_d \neq m_s$, and the Gell-Mann-Okubo relation can be used to eliminate the η mass.

10 Anomalous Lagrangian of $\mathcal{O}(p^6)$

The construction of the anomalous $\mathcal{O}(p^6)$ is a formidable task and was first completed for an arbitrary number of flavors (N_f) in 2001 by Bijmens et al. [11]. The only symmetries needed to construct the desired EQFT, are those of the initial and broken subgroup. One starts by listing all operators of a given order in the power expansion, compliant with all continuous and discrete symmetries. If we want to keep track of the phenomenologically relevant terms, it is imperative to reduce the list of operators to a minimum using all available constraints

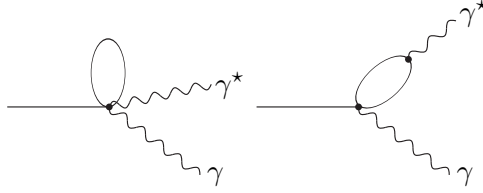


Figure 3: *One-loop diagrams for $PS \rightarrow \gamma\gamma^*$*

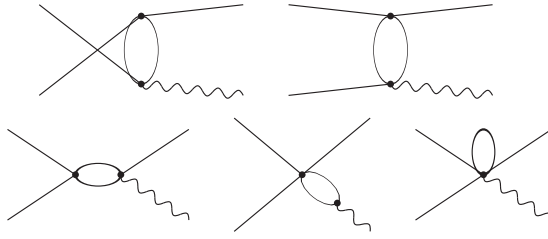


Figure 4: *One-loop diagrams for $\gamma\pi^0 \rightarrow \pi^+\pi^-$, $\eta \rightarrow \pi^+\pi^-\gamma$, $K^+ \rightarrow \pi^+\pi^-e^+\nu$ & $K^0 \rightarrow \pi^0\pi^0e^+\nu$*

and identities. The regularizing terms that cancel the infinite parts of the ultra-violet loop graphs contributing at $\mathcal{O}(p^6)$ must also be calculated.

10.1 Construction of the Effective Action

The following building blocks can be used in constructing monomials of $\mathcal{O}(p^6)$ in the chiral expansion: u_μ , $h_{\mu\nu} \equiv \nabla_\mu u_\nu + \nabla_\nu u_\mu$, $f_{\pm\mu\nu}$, $\chi_\pm \equiv u^\dagger \chi u^\dagger \pm u \chi u$. The motivation for using these is that they appear in the calculation of the divergent parts. Also, the number of terms built of these can easily be reduced to a minimum. QCD symmetry conditions of parity, charge conjugation and hermiticity must then be imposed on the list of operators. Since we are dealing with the anomalous sector the antisymmetric $\varepsilon^{\mu\nu\alpha\beta}$ enters, imposing further conditions.

Use of partial integration, antisymmetry conditions, the mathematical Bianchi & Schouten identities and the EOMs reduces the number of monomials to 24 for the general N_f case. In the three flavor case we use $SU(3)$ matrices obeying the Cayley-Hamilton relation, yielding an equation allowing for the removal of one more monomial. The Lagrangian density for $N_f = 3$ is then given by

$$\mathcal{L}_6^W = \sum_{i=1}^{23} C_i^W O_i^W \quad (82)$$

where the monomials O_i^W are listed in table 1. The infinities are removed using the \overline{MS} dimensional regularization scheme subtracting both infinite and omnipresent terms:

$$C_i^W = C_i^{Wr} + \eta_i \frac{\mu^{d-4}}{32\pi^2} \lambda \quad ; \lambda = \frac{2}{d-4} - \ln(4\pi) + \gamma_E - 1 \quad (83)$$

i	Monomial O_i^W	$384\pi^2 F^2 \eta_i$	i	Monomial O_i^W	$384\pi^2 F^2 \eta_i$
1	$i\varepsilon^{\mu\nu\alpha\beta} \langle \chi_- u_\mu u_\nu u_\alpha u_\beta \rangle$	12	13	$i\varepsilon^{\mu\nu\alpha\beta} \langle h_{\gamma\mu} \{f_{+\gamma\nu}, u_\alpha u_\beta\} \rangle$	-30
2	$\varepsilon^{\mu\nu\alpha\beta} \langle \chi_+ [f_{-\mu\nu}, u_\alpha u_\beta] \rangle$	-7	14	$i\varepsilon^{\mu\nu\alpha\beta} \langle h_{\gamma\mu} [f_{+\nu\alpha}, u_\gamma, u_\beta] \rangle$	-9
3	$\varepsilon^{\mu\nu\alpha\beta} \langle \chi_+ u_\mu \rangle \langle u_\nu f_{-\alpha\beta} \rangle$	-6	15	$i\varepsilon^{\mu\nu\alpha\beta} \langle h_{\gamma\mu} [u_\gamma, f_{+\nu\alpha}, u_\beta] \rangle$	3
4	$\varepsilon^{\mu\nu\alpha\beta} \langle \chi_- \{f_{+\mu\nu}, u_\alpha u_\beta\} \rangle$	-6	16	$\varepsilon^{\mu\nu\alpha\beta} \langle f_{-\gamma\mu} [u_\gamma, u_\nu u_\alpha u_\beta] \rangle$	18
5	$\varepsilon^{\mu\nu\alpha\beta} \langle \chi_- u_\mu f_{+\nu\alpha} u_\beta \rangle$	12	17	$\varepsilon^{\mu\nu\alpha\beta} \langle f_{-\mu\nu} [u_\gamma u_\gamma, u_\alpha u_\beta] \rangle$	15
6	$\varepsilon^{\mu\nu\alpha\beta} \langle \chi_- \rangle \langle f_{+\mu\nu} u_\alpha u_\beta \rangle$	8	18	$\varepsilon^{\mu\nu\alpha\beta} \langle f_{-\mu\nu} u_\alpha \rangle \langle u_\gamma u_\gamma u_\beta \rangle$	18
7	$i\varepsilon^{\mu\nu\alpha\beta} \langle \chi_- f_{+\mu\nu} f_{+\alpha\beta} \rangle$	0	19	$i\varepsilon^{\mu\nu\alpha\beta} \langle f_{+\gamma\mu} \{f_{-\gamma\nu}, u_\alpha u_\beta\} \rangle$	-12
8	$i\varepsilon^{\mu\nu\alpha\beta} \langle \chi_- \rangle \langle f_{+\mu\nu} f_{+\alpha\beta} \rangle$	0	20	$i\varepsilon^{\mu\nu\alpha\beta} \langle f_{+\gamma\mu} [f_{-\nu\alpha}, u_\gamma, u_\beta] \rangle$	-3
9	$i\varepsilon^{\mu\nu\alpha\beta} \langle \chi_- f_{-\mu\nu} f_{-\alpha\beta} \rangle$	0	21	$i\varepsilon^{\mu\nu\alpha\beta} \langle f_{+\gamma\mu} [u_\beta, f_{-\nu\alpha}, u_\gamma] \rangle$	15
10	$i\varepsilon^{\mu\nu\alpha\beta} \langle \chi_- \rangle \langle f_{-\mu\nu} f_{-\alpha\beta} \rangle$	0	22	$\varepsilon^{\mu\nu\alpha\beta} \langle u_\mu \{ \nabla_\gamma f_{+\gamma\nu}, f_{+\alpha\beta} \} \rangle$	12
11	$i\varepsilon^{\mu\nu\alpha\beta} \langle \chi_+ [f_{+\mu\nu}, f_{-\alpha\beta}] \rangle$	$-\frac{5}{2}$	23	$\varepsilon^{\mu\nu\alpha\beta} \langle u_\mu \{ \nabla_\gamma f_{-\gamma\nu}, f_{-\alpha\beta} \} \rangle$	0
12	$\varepsilon^{\mu\nu\alpha\beta} \langle h_{\gamma\mu} [u_\gamma, u_\nu u_\alpha u_\beta] \rangle$	-6			

Table 1: $\mathcal{O}(p^6)$ monomials & renormalization coefficients

where C_i^{Wr} are the renormalized coefficients, γ_E is the Euler constant, μ the arbitrary renormalization scale and d is the number of dimensions ($\rightarrow 4$). The coefficients η_i can be deduced from table 1. Once the infinite parts have canceled, we can solve for the renormalized coefficients C_i^{Wr} by experimental comparison. The triple (anti)commutators in table 1 are defined as

$$\begin{aligned} [a, b, c] &= abc - cba \\ \{a, b, c\} &= abc + cba \end{aligned}$$

We put the non-abelian field strengths in the operator $f_\pm^{\mu\nu} = u F_L^{\mu\nu} u^\dagger \pm u^\dagger F_R^{\mu\nu} u$.

10.2 Infinite parts

Calculating the second variation of the WZW & S_2 action ($\mathcal{O}(\xi^2)$ terms), and proceeding with dimensional regularization one obtains an expression for the divergent one-loop parts in arbitrary number of flavors (N_f) and colors (N_c).

$$\begin{aligned} Z_{1-loop}^{WZ\infty} &= -\frac{1}{16\pi^2(d-4)} \frac{N_c N_f}{1152\pi^2 F^2} \{ 4O_1^W + \left(-3 + \frac{6}{N_f^2}\right) O_2^W - \frac{6}{N_f} O_3^W - 2O_4^W \\ &\quad + 4O_5^W + \frac{8}{N_f} O_6^W + \left(-\frac{5}{6} + \frac{6}{N_f^2}\right) O_{11}^W - 2O_{12}^W - 10O_{13}^W - 3O_{14}^W + O_{15}^W \\ &\quad + 2O_{16}^W + O_{17}^W + \frac{6}{N_f} O_{18}^W - 4O_{19}^W - O_{20}^W + 5O_{21}^W + 4O_{22}^W - \frac{6}{N_f} O_{24}^W \} \end{aligned} \quad (84)$$

where the O_i^W are the monomials listed in table 1.

10.3 Example of Calculation

We continue with the $\pi^0 \rightarrow \gamma e^+ e^-$ decay. The fastest way to work yourself through the list is by counting the minimum number of fields a monomial must contribute. Then many of them

can quickly be discarded. We are looking for terms that can accommodate one meson and two photons. By rewriting operators in terms of vector (v_μ) and axial vector (a_μ) sources, we can quickly see which ones will contribute (since only v_μ contains the EM field). The most useful tools in simplifying expressions is partial integration and the anti-symmetry of $\varepsilon^{\mu\nu\alpha\beta}$.

$$\begin{aligned}
O_7^W &= i\varepsilon^{\mu\nu\alpha\beta} \langle \chi_- f_{+\mu\nu} f_{+\alpha\beta} \rangle = 64\sqrt{2} \frac{B_0 e^2}{F} \varepsilon^{\mu\nu\alpha\beta} \langle sMQ^2 \rangle \partial_\mu A_\nu \partial_\alpha A_\beta \\
&= \frac{64}{9} \frac{B_0 e^2}{F} (4m_u - m_d) \varepsilon^{\mu\nu\alpha\beta} \pi^0 \partial_\mu A_\nu \partial_\alpha A_\beta \\
O_8^W &= i\varepsilon^{\mu\nu\alpha\beta} \langle \chi_- \rangle \langle f_{+\mu\nu} f_{+\alpha\beta} \rangle = 64\sqrt{2} \frac{B_0 e^2}{F} \varepsilon^{\mu\nu\alpha\beta} \frac{1}{\sqrt{2}} (m_u - m_d) \pi^0 \langle Q^2 \rangle \partial_\mu A_\nu \partial_\alpha A_\beta \\
&= \frac{128}{3} \frac{B_0 e^2}{F} (m_u - m_d) \varepsilon^{\mu\nu\alpha\beta} \pi^0 \partial_\mu A_\nu \partial_\alpha A_\beta
\end{aligned}$$

O_{22}^W and O_{23}^W may contribute since the photon going to e^+e^- has $k_{\gamma^*}^2 \neq 0$. However,

$$f_\pm^{\mu\nu} \simeq F_L^{\mu\nu} \pm F_R^{\mu\nu} - [F_L^{\mu\nu}, m] \pm [F_R^{\mu\nu}, m] \equiv F_\pm^{\mu\nu} - \frac{i}{\sqrt{2}F} [F_\mp^{\mu\nu}, M]$$

to next-to-leading order in expanding the exponential, and $F_{+\mu\nu} \simeq 4\partial_\mu v_\nu$, $F_{-\mu\nu} \simeq -4\partial_\mu a_\nu$, so we can exclude O_{22}^W . For O_{23}^W we get

$$\begin{aligned}
O_{22}^W &= \varepsilon^{\mu\nu\alpha\beta} \langle u_\mu \{ \nabla_\gamma, f_{+\gamma\nu} f_{+\alpha\beta} \} \rangle \\
&= -\frac{4\sqrt{2}}{F} \varepsilon^{\mu\nu\alpha\beta} \langle \partial_\mu M (\partial_\gamma F_{L\gamma\nu} F_{L\alpha\beta} + F_{L\alpha\beta} \partial_\gamma F_{L\gamma\nu}) \rangle \\
&= 16\sqrt{2} \frac{e^2}{F} \varepsilon^{\mu\nu\alpha\beta} \langle MQ^2 \rangle \partial_\gamma^2 \partial_\mu A_\nu \partial_\alpha A_\beta \\
&= \frac{16}{3} \frac{e^2}{F} \varepsilon^{\mu\nu\alpha\beta} \pi^0 \partial_\gamma^2 \partial_\mu A_\nu \partial_\alpha A_\beta
\end{aligned}$$

Adding up the contributing monomials, we get the amplitude

$$\begin{aligned}
A(\pi^0 \gamma e^+ e^-) &= \frac{16}{9} \frac{e^3}{F} \varepsilon^{\mu\nu\alpha\beta} k_\mu \varepsilon_\nu k_\alpha^* \frac{\bar{e} \gamma_\beta e}{k_\alpha^{*2}} \times \\
&\quad (8B_0 (4m_u - m_d) C_7^W + 48B_0 (m_u - m_d) C_8^W - 3k^{*2} C_{22}^W) \quad (85)
\end{aligned}$$

The relations in section 4.3 can be used to rewrite the quark masses in terms of the pseudoscalar masses.

11 Models for the Chiral Coefficients

11.1 Vector Meson Dominance (VMD)

VMD is a phenomenologically very successful model that has not yet been derived from the standard model. It is based on the fact that higher mass resonances always enter the theory through virtual effects. VMD makes a dramatic appearance in the pion form factor, where the Breit-Wigner shape of the ρ meson can be seen.

The exchange of higher mass resonances can be used to estimate the finite part of the chiral coefficients. Roughly speaking, VMD states that for most processes, the main dynamic effect below the chiral breaking scale comes from the exchange of a vector meson. Using the hidden symmetry formulation by Bando et al. [22], and extending the formalism to include the anomalous sector J. Bijnens [3] has constructed an anomalous vector meson Lagrangian. Vector meson exchange can be described by including the ideally mixed ρ -nonet

$$\rho_\mu = \frac{1}{\sqrt{2}}\rho_\mu^a\lambda^a + \frac{1}{\sqrt{3}}\rho_\mu^1 \quad (86)$$

in a chiral invariant way. Operator strings with the correct symmetry properties can be constructed using the covariant and hermitian building blocks $\rho_{\mu\nu} = \partial_\mu\rho_\nu - \partial_\nu\rho_\mu + ig[\rho_\mu, \rho_\nu]$, $\xi^\dagger\ell_{\mu\nu}\xi$, $\xi r_{\mu\nu}\xi$, where $\xi = \exp iM/F\sqrt{2}$. The coupling g can be determined from the $\rho \rightarrow \pi\pi$ width.

The heavy ρ -meson nonet, consisting of $\rho^{\pm,0}$, $K^{\pm,0}$, $\bar{K}^{*,0}$, ω & ϕ , will only enter virtually and can be integrated out, assuming that their masses are much greater than the momenta. The resulting expression will contain parameters that can be constrained by comparing with the radiative decay widths of vector mesons. We will not list the full anomalous vector Lagrangian here - the reader is referred to [3] for further details. As an example, coefficients can be chosen such that one obtains a Lagrangian describing direct $\rho\rho M$ interaction (where M stands for a pseudoscalar meson).

$$\mathcal{L}(\rho_\mu \rightarrow \rho_\mu M) = \frac{3}{4\pi^2} \frac{g^2}{\sqrt{2}F} \varepsilon^{\mu\nu\alpha\beta} \text{tr}(\partial_\mu\rho_\nu\partial_\alpha\rho_\beta M) \quad (87)$$

This Lagrangian can be used to calculate the $M \rightarrow \gamma\gamma^*$ amplitudes via the $\rho\rho$ resonance: $M \rightarrow \rho\rho \rightarrow \gamma\gamma^*$. To obtain the connection with ℓ_μ and r_μ one must first integrate out the ρ resonance. It should be noted that it is also possible to calculate the $\rho\rho M$ amplitude using an ordinary Feynman diagram approach. Integrating out the vector mesons one then obtains the effective Lagrangian for $M \rightarrow \gamma\gamma^*$ processes:

$$\begin{aligned} \mathcal{L}_6^{M \rightarrow \gamma\gamma^*} = & \dots - i \frac{e^2}{4M_\rho^2} \frac{3}{8\pi^2} \varepsilon^{\mu\nu\alpha\beta} F_{\alpha\beta} \partial^\lambda F_{\lambda\nu} \\ & \times \left\langle Q^2 \Sigma^\dagger \partial_\mu \Sigma - Q^2 \Sigma \partial_\mu \Sigma^\dagger + Q \Sigma^\dagger Q \partial_\mu \Sigma - Q \Sigma Q \partial_\mu \Sigma^\dagger \right\rangle \end{aligned}$$

where $F_{\mu\nu}$ is the EM field strength tensor, $Q = \frac{1}{3} \text{diag}(2, -1, -1)$ and $\Sigma = \exp(i\sqrt{2}M/F)$. Similar $\mathcal{O}(p^6)$ VMD expressions can be obtained for the other anomalous processes.

11.2 Chiral Constituent Quark Model (CQM)

The constituent quark model is based on the assumption that vertices has to come from constituent quark loops. This effect is merged with the chiral formalism by including the constituent quarks in a chiral invariant way. Here follows a brief introduction to the model, for a more in-depth and technical analysis the reader is referred to Bijnens [3] or Ball [23]. The euclidean space Lagrangian density can be written

$$\mathcal{L} = \mathcal{L}_{QCD} + \mathcal{L}_M = \bar{q}\mathcal{D}q \quad (88)$$

where

$$\begin{aligned} \mathcal{D} = \gamma_\mu D_\mu + \mathcal{M} & \quad ; \quad D_\mu = \partial_\mu + ig_S G_\mu + i\ell_\mu P_L + ir_\mu P_R \\ & \quad ; \quad \mathcal{M} = -m_Q \left(U^\dagger P_L + U P_R \right) \end{aligned} \quad (89)$$

where m_Q is the constituent quark mass. We neglect gluonic corrections and will consequently drop G_μ in (89). This is a large distance QCD approximation that will reproduce the anomaly correctly and is expected to work reasonably well. A connection with the effective approach in terms of the GS bosons can be obtained by integrating out the quarks.

$$e^{\Gamma(U, \ell_\mu, r_\mu)} = \int [d\bar{q}][dq] e^{\int d^4x \mathcal{L}_{QCD}} \Rightarrow \quad (90)$$

$$\Gamma = \log \det \mathcal{D} = \text{tr} \log \mathcal{D} \quad (91)$$

and similarly for Γ^* replacing \mathcal{D} with \mathcal{D}^\dagger . The determinant corresponds to a trace over color, flavor, Dirac indices and space-time. With Γ^* and Γ we can obtain a real part Γ^+ and imaginary part Γ^- . It should be emphasized that this is only possible since we're working in euclidean space. In the physical Minkowski space-time imaginary parts are not allowed. Since we are ultimately interested in the anomalous sector, we evaluate the effect of the intrinsic parity operation, and find that $\Gamma^\pm \rightarrow \pm \Gamma^\pm$. This means that Γ^+ contains an even and Γ^- an odd number of $\varepsilon^{\mu\nu\alpha\beta}$. In order to preserve the ordinary and break the intrinsic parity symmetry we know that we must have an odd power of $\varepsilon^{\mu\nu\alpha\beta}$. (91) gives

$$\Gamma^- = -\log \det \mathcal{D}^\dagger \quad (92)$$

This can be manipulated to obtain the correct expression describing the anomalous sector. The process involves rewriting (92) on a five-dimensional integral with four-dimensional space-time boundaries, singling out $\varepsilon^{\mu\nu\alpha\beta}$ -terms and expanding in m_Q . All but the WZW terms will be suppressed by the constituent quark mass. In order to perform the integration over the extra time-like dimension (c.f. τ in WZW section), one can then make a Seeley-DeWitt expansion, singling out the contributing terms with SDW coefficients a_i .

In this thesis we want to test the CQM $\mathcal{O}(p^6)$ predictions by comparing them to the chiral $\mathcal{O}(p^6)$ coefficients fixed by experiment. We will thus focus on the $\mathcal{O}(p^6)$ abnormal intrinsic parity effective action. The Γ^+ describing the normal parity sector, can also produce anomalous terms. This is because the EOMs have been used in rewriting Γ^+ , and these contain both anomalous and non-anomalous parts. However, this type of terms can be shown to be of $\mathcal{O}(p^8)$ and are not of interest here. The final result involves the contribution of terms with Seely-DeWitt coefficients a_3 (describing one external field and 3 PS mesons), a_4 (2 external vector fields and one PS meson) and a_5 (5 PS interaction). The explicit form of $\sum_{i=3,4,5} \Gamma^-(a_i)$ is very lengthy and can be found in appendix B.

12 Results

12.1 Combining Amplitudes

We are now ready to combine all the amplitudes: the WZW $\mathcal{O}(p^4)$, the one-loops and the $\mathcal{O}(p^6)$ terms. Following through with the example of the $\pi^0 \rightarrow \gamma e^+ e^-$ decay, we can verify that the divergent part of the loops are canceled by the parameters of $\mathcal{O}(p^6)$. This serves a

test for consistent calculations. Combining (78) & (85) with the loop amplitude in appendix A we get

$$\begin{aligned}
A^{an} &= A_{WZW} + A_{1\ell} + A_6 = \frac{1}{4\pi^2} \frac{e^3}{F_\pi} \varepsilon^{\mu\nu\alpha\beta} \varepsilon_\mu k_\nu \frac{\bar{e}\gamma_\alpha e}{k^{\star 2}} k_\beta^\star \times \\
&\quad [1 + \frac{1}{32\pi^2 F^2} \{ \frac{2}{3} \lambda k^{\star 2} - \frac{1}{3} k^{\star 2} (\log \frac{m_K^2}{\mu^2} + \log \frac{m_\pi^2}{\mu^2}) + \frac{10}{9} k^{\star 2} \\
&\quad + \frac{4}{3} [F(k^{\star 2}, m_\pi^2) + F(k^{\star 2}, m_K^2)] \} - \frac{512}{9} B_0 (4m_u - m_d) \pi^2 C_7^{Wr} \\
&\quad - \frac{1024}{3} B_0 (m_u - m_d) \pi^2 C_8^{Wr} + k_\gamma^{\star 2} \left(\frac{64}{3} \pi^2 C_{22}^{Wr} - \frac{1}{48\pi^2 F^2} \mu^{d-4} \lambda \right)]
\end{aligned}$$

We see that the infinite parts cancel: $A^\lambda = \frac{1}{32\pi^2 F^2} \frac{2}{3} \lambda k^{\star 2} - \frac{1}{48\pi^2 F^2} \mu^{d-4} \lambda k^{\star 2} = 0$. The function F comes from the evaluation of the loop integrals and can be found in appendix A.

12.2 Theoretical Quantum Field Calculations

The results of the theoretical calculations are displayed in table 2, where the first term in the brackets is due to the WZW action. For the sake of completeness the one-loop contributions $A_{1\ell}$ are listed in appendix A.

PROCESS:	AMPLITUDE:
$\pi^0 \rightarrow \gamma\gamma$	$ \begin{aligned} &\frac{\alpha}{\pi F_\pi} \varepsilon^{\mu\nu\alpha\beta} \varepsilon_\mu k_\nu \varepsilon_\alpha^\star k_\beta^\star \times \\ &[1 - \frac{128}{9} \pi^2 (20m_K^2 + m_\pi^2 - 15m_\eta^2) C_7^{Wr} \\ &- 12 \frac{128}{9} \pi^2 (4m_K^2 - m_\pi^2 - 3m_\eta^2) C_8^{Wr}] \end{aligned} $
$\eta \rightarrow \gamma\gamma$	$ \begin{aligned} &\frac{\alpha}{\sqrt{3}\pi F_\eta} \varepsilon^{\mu\nu\alpha\beta} \varepsilon_\mu k_\nu \varepsilon_\alpha^\star k_\beta^\star \times \\ &[1 - \frac{128}{3} (4m_K^2 - 5m_\eta^2 + 3m_\pi^2) \pi^2 C_7^W + 512 (m_\pi^2 - m_\eta^2) \pi^2 C_8^W] \end{aligned} $
$\pi^0 \rightarrow \gamma e^+ e^-$	$ \begin{aligned} &\frac{1}{4\pi^2} \frac{e^3}{F_\pi} \varepsilon^{\mu\nu\alpha\beta} \varepsilon_\mu k_\nu \frac{\bar{e}\gamma_\alpha e}{k^{\star 2}} k_\beta^\star \times \\ &[1 - \frac{256}{3} \pi^2 m_\pi^2 C_7^{Wr} + \frac{64}{3} \pi^2 k^{\star 2} C_{22}^{Wr}] + A_{\pi^0 \gamma e^+ e^-}^{1\ell} \end{aligned} $
$\eta \rightarrow \gamma e^+ e^-$	$ \begin{aligned} &\frac{e^3}{4\sqrt{3}\pi^2 F_\eta} \varepsilon^{\mu\nu\alpha\beta} \varepsilon_\mu k_\nu \frac{\bar{e}\gamma_\alpha e}{k^{\star 2}} k_\beta^\star \times \\ &[1 - \frac{128}{9} \pi^2 (12m_K^2 - 15m_\eta^2 + 9m_\pi^2) C_7^{Wr} - 36 \frac{128}{9} \pi^2 (m_\pi^2 - m_\eta^2) C_8^{Wr} \\ &+ \frac{192}{9} \pi^2 k^{\star 2} C_{22}^{Wr}] + A_{\eta \gamma e^+ e^-}^{1\ell} \end{aligned} $

$\pi^+ \rightarrow \gamma e^+ \nu$	$\frac{eG_F \cos \theta}{8\pi^2 F_\pi} \varepsilon^{\mu\nu\alpha\beta} l_\mu q_\nu \varepsilon_\alpha k_\beta \times$ $\left[1 - \frac{256}{3} \pi^2 m_\pi^2 C_7^{Wr} + \frac{64}{3} \pi^2 (q^2 + k^2) C_{22}^{Wr}\right] + A_{\pi^+ \gamma e^+ \nu}^{1\ell}$
$K^+ \rightarrow \gamma e^+ \nu$	$\frac{eG_F \sin \theta}{8\pi^2 F_K} \varepsilon^{\mu\nu\alpha\beta} l_\mu q_\alpha \varepsilon_\beta k_\beta \times$ $\left[1 - \frac{256}{3} \pi^2 m_K^2 C_7^{Wr} + 256 \pi^2 (m_K^2 - m_\pi^2) C_{11}^{Wr} + \frac{64}{3} \pi^2 (q^2 + k^2) C_{22}^{Wr}\right]$ $+ A_{K^+ \gamma e^+ \nu}^{1\ell}$
$\gamma \pi^0 \rightarrow \pi^+ \pi^-$	$\frac{1}{4\pi^2} \frac{e}{F_\pi^3} \varepsilon^{\mu\nu\alpha\beta} \varepsilon_\mu p_\nu p_\alpha p_\beta \times$ $\left[1 + 64 \pi^2 m_\pi^2 (2C_4^{Wr} + C_5^{Wr} - C_{14}^{Wr} - C_{15}^{Wr})\right.$ $\left. + \frac{64}{3} \pi^2 k^2 (C_{14}^{Wr} + C_{15}^{Wr} - C_{13}^{Wr})\right] + A_{\gamma \pi^0 \pi^+ \pi^-}^{1\ell}$
$\eta \rightarrow \gamma \pi^+ \pi^-$	$\frac{1}{4\pi^2 \sqrt{3}} \frac{e}{F_\pi^2 F_{\eta 8}} \varepsilon^{\mu\nu\alpha\beta} \varepsilon_\mu p_\nu p_\alpha^{\pi^+} p_\beta^{\pi^-} \times$ $\left[1 + 192 \pi^2 (m_\pi^2 - m_\eta^2) (C_6^{Wr} - C_3^{Wr})\right.$ $+ \frac{32}{3} \pi^2 (4m_K^2 - 3m_\eta^2 + 5m_\pi^2) (C_5^{Wr} + 2C_4^{Wr})$ $+ 128 \pi^2 p_+ p_- C_{15}^{Wr} - 128 \pi^2 [p_\eta p_+ + p_\eta p_- + p_+ p_-] C_{14}^{Wr}$ $+ 64 \pi^2 [p_\eta p_+ + p_\eta p_- - m_\eta^2] C_{13}^{Wr}] + A_{\gamma \eta 8 \pi^+ \pi^-}^{1\ell}$
$K^+ \rightarrow \pi^+ \pi^- e^+ \nu$	$\frac{G_F \sin \theta}{4\pi^2 F_\pi^2 F_K} \varepsilon^{\mu\nu\alpha\beta} l_\mu q_\nu p_\alpha^+ p_\beta^- \times$ $\left[1 + 64 \pi^2 (m_K^2 - m_\pi^2) C_2^{Wr} + 32 \pi^2 (3m_\pi^2 - 2m_K^2) C_4^{Wr}\right.$ $+ 64 \pi^2 m_\pi^2 C_5^{Wr} - 32 \pi^2 q (q + p_+) C_{13}^{Wr} - 128 \pi^2 p_- p_K C_{14}^{Wr}$ $\left. - 64 \pi^2 p_+ (q + p_+) C_{15}^{Wr}\right] + A_{K^+ \pi^+ \pi^- e^+ \nu}^{1\ell}$
$K^+ \rightarrow \pi^0 \pi^0 e^+ \nu$	$\frac{G_F \sin \theta}{4\pi^2 F_K F_\pi^2} \varepsilon^{\mu\nu\alpha\beta} l_\mu q_\nu p_\alpha p_\beta \times$ $(p_{\pi_1^0} - p_{\pi_2^0}) [-16 \pi^2 q C_{13}^{Wr} + 64 \pi^2 p_K C_{14}^{Wr} + 32 \pi^2 p_K C_{15}^{Wr}]$ $+ A_{K^+ \pi^0 \pi^0 e^+ \nu}^{1\ell}$

Table 2: *Results of theoretical quantum field calculations.*

k stands for the photon and q for the di-lepton four-momentum. The other momenta have

been labeled as needed. The W_μ has been replaced with the leptonic current

$$W_\mu \rightarrow \frac{g}{2\sqrt{2}M_W^2} l_\mu \equiv \frac{g}{2\sqrt{2}M_W^2} \bar{u}_\nu \gamma_\mu (1 - \gamma_5) v_e$$

with $G_F/\sqrt{2} = g^2/8M_W^2$. In the $M \rightarrow \gamma\gamma^*$ decays, note the absence of loop corrections in the case of real photons. It is interesting to see that the kinetic part of the electroweak fields in the decays with one pseudoscalar and two external fields are all connected to the C_{22}^{Wr} coefficient. From experiment we expect this chiral coefficient to be rather large with respect to the others in the decay amplitude. C_{22}^{Wr} obviously becomes increasingly significant at higher energies, so it is important to extract a good value. In the cases where they are active, C_{13}^{Wr} , C_{14}^{Wr} and C_{15}^{Wr} play a similar role - they are also connected to kinematical factors, but do not vanish in the soft limit. Inspecting the corresponding monomials in table 1, we can trace the kinematical dependence to the presence of an extra ∂_γ 4-derivative. Other monomials have the same property but forcably contain a minimum of fields that exceeds the number allowed by the process.

The Gell-Mann-Okubo relation has been used to eliminate the η_8 mass in all processes except for those involving an η . Terms connected to C_8^{Wr} in $\pi^0\gamma e^+e^-$ and to C_{11}^{Wr} in $\pi^0\gamma e^+\nu$ are proportional to $m_u - m_d$, and do not appear in table 2 since we are working in the isospin limit. The loop corrections must be recalculated if we wish evaluate the amplitudes away from the isospin limit.

In all processes containing an on-shell photon, the term proportional to k^2 has been kept, even though this will be set to zero when comparing with the experimental data. Such terms will become useful when we are comparing with the VMD & CQM predictions.

12.3 Experimental Comparison

Experimental data in the form of slopes, form factors and decay rates will allow us to extract numerical values for the chiral coefficients. The slope parameter b is defined as

$$b = \frac{1}{A(M \rightarrow \gamma\gamma)} \frac{d}{dk^2} A(M \rightarrow \gamma\gamma^*)|_{k^*=0} \quad (93)$$

i.e. the factor in front of the off-shell photon squared four-momentum, normalized by the on-shell amplitude. To calculate the width we make use of the standard formula for two body decays, except in the case of $\gamma\eta\pi^+\pi^-$ where it's necessary to perform three body phase space integration. The form factors allow for easy comparison, as they can be directly related to the matrix element. Below, all cases are treated individually - the results are summarized in table 3. The coefficients have been solved for using the least square solver in the MINUIT program (part of the CERN programming resource library). The errors are mainly due to experimental uncertainty, but all error limits have a contribution coming from the decay constants, of which we still have relatively poor knowledge. Measurements on charged pion decays give $F_\pi = 92.4 \pm 0.33\text{MeV}$. Next-to-leading order values for the other decay constants can be extracted through wavefunction renormalization as in [3]. Many sources use an alternative convention and quote $f_M = \sqrt{2}F_M$.

12.3.1 $\pi^0/\eta \rightarrow \gamma\gamma^*$

For real photons we form the decay rate by squaring the matrix element and tagging it with the appropriate factors. The squaring involves inserting one half for identical photons and then

<i>Process:</i>	<i>Experimental input:</i>	<i>Solved Coefficients</i> [10^{-9}MeV^{-2}]
$\pi^0 \rightarrow \gamma\gamma$ & $\eta \rightarrow \gamma\gamma$	Width [18] Width [18]	$C_7^{Wr} \simeq 0.013 \pm 1.17$ $C_8^{Wr} \simeq 0.76 \pm 0.18$
$\pi^0 \rightarrow \gamma e^+ e^-$	Slope parameter [24]	$C_{22}^{Wr} \simeq 6.52 \pm 0.78$
$\eta \rightarrow \gamma e^+ e^-$	Slope parameter [24]	$C_{22}^{Wr} \simeq 5.07 \pm 0.71$
$\pi^+ \rightarrow \gamma e^+ \nu$	Form factor [18]	$C_7^{Wr} \simeq 20.3 \pm 18.7$
$K^+ \rightarrow \gamma e^+ \nu$	Form factor [18]	$C_{11}^{Wr} \simeq -6.37 \pm 4.54$
$\gamma\pi^0\pi^+\pi^-$ & $K^+ \rightarrow \pi^+\pi^-e^+\nu$	Form factor [28] Form factors [25]	$C_2^{Wr} \simeq -0.32 \pm 10.4$ $C_4^{Wr} \simeq 0.28 \pm 9.19$ $C_5^{Wr} \simeq 28.50 \pm 28.83$ $C_{13}^{Wr} \simeq -74.09 \pm 55.89$ $C_{14}^{Wr} \simeq 29.99 \pm 11.14$ $C_{15}^{Wr} \simeq -25.30 \pm 23.93$
$\eta\gamma\pi^+\pi^-$	Width [18]	$C_3^{Wr} - C_6^{Wr} \simeq 21.67 \pm 17.41$
$K^+ \rightarrow \pi^0\pi^0e^+\nu$	NA	

Table 3: *Solved coefficients*

summing over all polarizations as in section 8.2. Width data is quoted in [18] as a weighted average of several measurements, yielding $\Gamma_{\pi^0\gamma\gamma} = 7.836 \pm 0.523$ eV and $\Gamma_{\eta\gamma\gamma} = 465 \pm 44$ eV respectively. Note that the calculation was performed with the Goldstone boson matrix (11), i.e. using η_8 . Instead of explicitly implementing the mixing model of section 6, we conveniently let the chiral coefficients supply the needed extra factor. Proceeding in this way we are left with two equations, allowing us to solve for C_7^{Wr} and C_8^{Wr} .

For on-shell photons we can extract C_{22}^{Wr} using (93). To this end, we use the results of the CLEO II detector differential cross section measurements [24]. Fitting the form factor data they arrive at the pole parameters $\Lambda_{\pi^0} = 776 \pm 38\text{MeV}$ ($= b^{-1/2}$) and $\Lambda_\eta = 774 \pm 49\text{MeV}$. The similar slopes indicate that the two meson wavefunctions are nearly identical. Looking at table 3 we see that the two extracted values for C_{22}^{Wr} agree within the error limits. Also note that C_{22}^{Wr} is an order of magnitude larger than C_7^{Wr} and C_8^{Wr} .

12.3.2 $\pi^+/K^+ \rightarrow \gamma e^+ \nu$

For these decays the Particle Data Group [18] quotes constant vector form factors (F_V), as no momentum dependence can be seen in the region of the experiments. The axial current is not of interest here as it belongs to the non-anomalous sector. Experimental vector form factor measurements yield the matrix element

$$M(SD_V) = \frac{eG_F V_{qq'}}{\sqrt{2}m_P} \varepsilon^\mu l^\nu F_V^\pi \varepsilon_{\mu\nu\sigma\tau} k^\sigma q^\tau \quad ; F_V^\pi = (0.017 \pm 0.008) \quad (94)$$

Comparing with the pion amplitude in table 2 we find

$$F_V^\pi = \frac{m_{\pi^+}^2}{4\sqrt{2}\pi^2 F_\pi} \times [1 + \frac{1}{32\pi^2 F_\pi^2} \{-4m_\pi^2 \ln \frac{m_\pi^2}{\mu^2} - 4m_K^2 \ln \frac{m_K^2}{\mu^2} + 4I(q^2, m_\pi^2, m_\pi^2) + 4I(k^2, m_\pi^2, m_K^2)\} - \frac{256}{3}\pi^2 m_\pi^2 C_7^{Wr} + \frac{64}{3}\pi^2 (q^2 + k^2) C_{22}^{Wr}] \quad (95)$$

where the one-loop corrections from appendix A have been inserted. Setting the photon and dilepton four-momenta squared (k^2 and q^2 respectively) to zero, allows solving for C_7^{Wr} . The measurements are rather imprecise, so the extracted value for C_7^{Wr} should simply be regarded as an upper limit. The $M \rightarrow \gamma\gamma^*$ value is closer to the truth. As for C_{11}^{Wr} , this coefficient can only be extracted from the K^+ decay, or alternatively from the π^+ decay recalculated away from the isospin limit. Considering the poor data presently available, the recalculation hardly seems worth the effort. Repeating the above procedure for the kaon, with $F_V^K = (0.204 \pm 0.070)$, we can extract a value for C_{11}^{Wr} . The fact that this value is negative is not a problem, since there is nothing in the theory which contradicts negative values for the chiral coefficients.

12.3.3 $\gamma\pi^0\pi^+\pi^-$

Experimental data [28] does not reveal any kinematical dependence. The amplitude is expressible in terms of the $\gamma 3\pi$ coupling constant $F^{3\pi} = 12.9 \pm 1.4 \text{ GeV}^{-3}$. Parsing the amplitude from table 2 and the loop corrections from appendix A, we set $k^2 = 0$ and the invariant $p_{ij}^2 = (p_i + p_j)^2$ to their average value - one third into their respective kinematical range.

$$\begin{aligned} -3.5m_\pi^2 \leq p_{01}^2 \equiv (p_{\pi^0} - p_{\pi^-})^2 \leq 0 &\Rightarrow \langle p_{01}^2 \rangle \simeq -\frac{7}{6}m_\pi^2 \\ 4m_\pi^2 \leq p_{02}^2 \equiv (p_{\pi^0} - p_{\pi^+})^2 \leq 13m_\pi^2 &\Rightarrow \langle p_{02}^2 \rangle \simeq 7m_\pi^2 \\ \sum p_{ij}^2 = \sum m_i^2 &\Rightarrow \langle p_{12}^2 \rangle = -\frac{17}{6}m_\pi^2 \end{aligned}$$

This gives

$$\begin{aligned} F^{3\pi} \simeq & \sqrt{\frac{\alpha}{4\pi}} \frac{1}{\pi F_\pi^3} \times [1 + \frac{1}{96\pi^2 F^2} \{-3m_\pi^2 \log \frac{m_\pi^2}{\mu^2} + 5m_\pi^2 \\ & + 4F(m_\pi^2, -\frac{17}{6}m_\pi^2) + 4F(m_\pi^2, 7m_\pi^2) + 4F(m_\pi^2, -\frac{7}{6}m_\pi^2)\} \\ & - 64\pi^2 m_\pi^2 [C_{14}^{Wr} + C_{15}^{Wr} - 2C_4^{Wr} - C_5^{Wr}]] \end{aligned} \quad (96)$$

producing one equation with the unknown combination $(C_{14}^{Wr} + C_{15}^{Wr} - 2C_4^{Wr} - C_5^{Wr})$. What we have done is clarified in figure 5, where the theoretical form factor and $F^{3\pi}$ have been plotted as functions of p_{01}^2 and p_{12}^2 in units of m_π^2 . We have simply aligned the form factor average with the experimentally observed, constant plane $F^{3\pi}$. Note that the error on $F^{3\pi}$ transcends the maximum deviation of the theoretical surface from the plane.

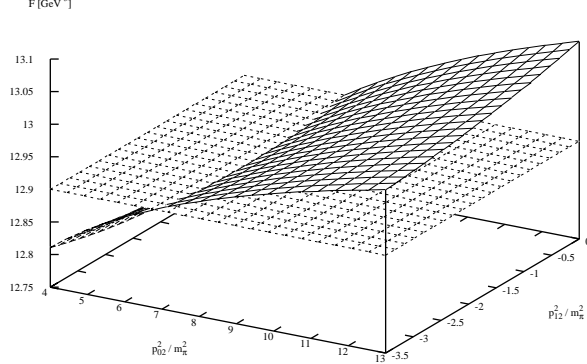


Figure 5: *Experimental (dashed) & theoretical (solid) form factor.*

12.3.4 $\eta\gamma\pi^+\pi^-$

To compare with available data in the form of the decay rate $\Gamma_{\eta\gamma\pi\pi} = 55.2 \pm 6.6$ eV [18], we must perform three-body phase space integration. We make use of the formula

$$d\Gamma = \frac{1}{(2\pi)^3} \frac{1}{32m_\eta^3} |\mathcal{M}|^2 dp_{12}^2 dp_{23}^2 \quad (97)$$

by rewriting the amplitude in terms of the invariants $p_{12}^2 \equiv (p_+ + p_-)^2$ and $p_{23}^2 \equiv (p_- + k)^2$ and evaluating the integral numerically. The final result is an equation with chiral coefficients 4-6 and 13-14 as unknowns. This equation contains a term proportional to $C_3^{Wr} - C_6^{Wr}$. Since these coefficients only appear in $\eta\gamma\pi\pi$, they cannot be solved for individually, and all we can do is to extract a value for the difference between them.

12.3.5 $K^+ \rightarrow \pi^+\pi^-e^+\nu$

This decay provides the best experimental data in the form of an energy dependent vector form factor. Data from 4×10^5 events were recently (2001) collected at the Brookhaven Alternating Gradient Synchrotron [25] over a broad kinematical range. The matrix element is quoted as

$$M = \frac{G_F}{\sqrt{2}} V_{us}^* \bar{u}(p_\nu) \gamma_\mu (1 - \gamma_5) v(p_e) (V^\mu - A^\mu) \quad (98)$$

where we only concern ourselves with the hadronic vector contribution $V^\mu = H \varepsilon^{\mu\nu\rho\sigma} L_\nu P_\rho Q_\sigma$, with $P = p_+ + p_-$, $Q = p_+ - p_-$, $L = p_e + p_\nu$ in units of m_K and where the dimensionless H is a function of the invariant dipion mass $M_{\pi\pi} = |p_+ + p_-|$. 6 datapoints for H are quoted in the range $280\text{MeV} \leq M_{\pi\pi} \leq 380\text{MeV}$. No angular dependence was detected in this energy range. Comparing (98) with the amplitude in table 3, we can extract 6 equations with $H(M_{\pi\pi}^2, (p_K - p_+)^2, (p_K - p_-)^2)$. This requires rewriting the matrix element using relativistic kinematics and verifying that the dependence on θ_π (the polar angle of the π^+ with respect

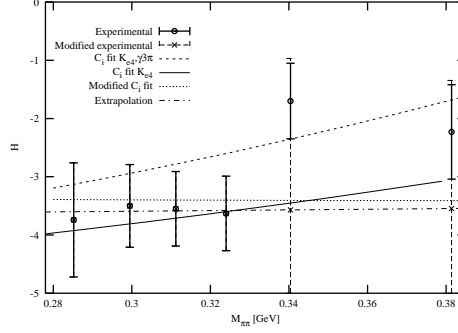


Figure 6: *Experimental & chiral predictions of H .*

to the dipion in the kaon rf) is small. Let the z axis be parallel to the dipion flight direction. In the kaon restframe we have

$$\begin{aligned} p_K &= (m_K, \mathbf{0}) \\ p_{2\pi} &= (\sqrt{M_{\pi\pi}^2 + |\mathbf{p}_{2\pi}|^2}, 0, 0, |\mathbf{p}_{2\pi}|) \end{aligned}$$

where $|\mathbf{p}_{2\pi}| \simeq (m_K^2 - M_{\pi\pi}^2)^2 / m_K$ with $q^2 \simeq 0$. In the dipion restframe we have

$$\begin{aligned} p_{2\pi} &= (E_{2\pi}, 0, 0, 0) \\ p_+ &= (\tfrac{1}{2}E_{2\pi}, 0, p_\pi \sin \theta_\pi, p_\pi \cos \theta_\pi) \quad ; p_\pi = \sqrt{\tfrac{1}{4}M_{\pi\pi}^2 - m_\pi^2} \\ p_- &= (\tfrac{1}{2}E_{2\pi}, 0, -p_\pi \sin \theta_\pi, -p_\pi \cos \theta_\pi) \\ p_K &= (E_K, 0, 0, -|\mathbf{p}_K|) \end{aligned}$$

where we can extract E_K and $|\mathbf{p}_K|$ using the frame invariance of scalars: $p_K^{Krf} p_{2\pi}^{Krf} = p_K^{2\pi rf} p_{2\pi}^{2\pi rf}$. We can now recast the amplitude in the appropriate form and verify that the angular dependence is small. For example:

$$p_K p_- = \tfrac{1}{4} (m_K^2 + M_{\pi\pi}^2) - \frac{(m_K^2 - M_{\pi\pi}^2)}{2M_{\pi\pi}} \sqrt{\tfrac{1}{4}M_{\pi\pi}^2 - m_\pi^2} \cos \theta_\pi \quad (99)$$

The second term becomes very small when $M_{\pi\pi} \simeq m_K$ or $4m_\pi$. In addition, the term is suppressed by $M_{\pi\pi}$ and the cos factor.

The 6 extracted equations, involving coefficients 2, 4, 5 and 13-15, are now merged with the equation from $\gamma 3\pi$, giving a total of 7 equations with 6 unknowns. This system is over-determined, which will help to reduce the errors.

The data series has been plotted in figure 6, along with the prediction of the fitted chiral parameters. Evidently the data points at the high end of the spectrum deviates significantly from the prediction. It is unclear whether or not this is just a statistical fluke, or if it originates somewhere in the experimental setup. The dominating accidental background was from $K\pi^0\pi^+\pi^-$, with a $\pi^+\pi^-$ pair detection along with an e^+ from the beam or coincident decay. However, this was reduced to $2.4 \pm 1.2\%$ using a likelihood method.

If we hypothesize that the deviating points are indeed due to a statistical fluke, this can be compensated for by extrapolating a line using the first four data points to the high energy

<i>Process:</i>	$C_i^{Wr} [10^{-9} \text{ MeV}^{-2}]$
$K^+ \rightarrow \pi^+ \pi^- e^+ \nu$	$C_2^{Wr} \simeq 0.78 \pm 12.7$ $C_4^{Wr} \simeq 0.67 \pm 10.9$ $C_5^{Wr} \simeq 9.38 \pm 152.2$ $C_{13}^{Wr} \simeq -8.44 \pm 69.9$ $C_{14}^{Wr} \simeq 0.72 \pm 15.3$ $C_{15}^{Wr} \simeq -3.10 \pm 28.6$
$\eta \rightarrow \gamma \pi^+ \pi^-$	$C_3^{Wr} - C_6^{Wr} \simeq 4.6 \pm 26.6$

Table 4: *Coefficient values as a result of extrapolation.*

<i>process:</i>	<i>Amplitude:</i>	<i>source:</i>
$\pi^0 (\eta) \rightarrow \gamma e^+ e^-$	$\frac{k^2}{M_\rho^2}$	[3]
$\pi^+ (K^+) \rightarrow \gamma e^+ \nu$	$\frac{1}{M_\rho^2} (k^2 + q^2)$	[21]
$\gamma \pi^0 \rightarrow \pi^+ \pi^-$	$\frac{1}{2M_\rho^2} (p_{01}^2 + p_{02}^2 + p_{12}^2 + 3k^2)$	[26]
$\eta_8 \gamma \rightarrow \pi^+ \pi^-$	$\frac{3}{2M_\rho^2} (p_{12}^2 + k^2)$	[26]
$K^+ \pi^+ \pi^- e^+ \nu$	$\frac{3}{4M_\rho^2} (2q^2 + (p_+ + p_-)^2 + (q + p_-)^2)$	[21]

Table 5: *VMD $\mathcal{O}(p^6)$ predictions.*

region. Also, we exclude the $\gamma 3\pi$ equation as the measurement is not very good. Proceeding in this way, we can refit the chiral coefficients, producing a radically altered slope (see figure 6) and the C_i s in table 4. The errors have been overestimated, reflecting the uncertainty in the extrapolation procedure. This is why the errors in table 4 have been inflated.

12.4 VMD Comparison

VMD is unable to predict the mass terms of the chiral theory, as the Lagrangian contains no explicit mass parameters. Table 5 shows the $\mathcal{O}(p^6)$ VMD expressions that should be compared with the chiral predictions. The prefactors are the same as for the $\mathcal{O}(p^6)$ chiral expressions, allowing for direct comparison with the terms proportional to kinematical factors.

The $M \rightarrow \gamma \gamma^*$ contains no kinematical dependence for on-shell photons. For off-shell photons π^0 and η give the same result:

$$C_{22}^{Wr} = \frac{3}{64M_\rho^2\pi^2} \simeq 8.01 \times 10^{-9} \text{ MeV}^{-2}$$

in excellent agreement with the result in table 3. $\pi^+ (K^+) \gamma e^+ \nu$ offers no new constraints.

	VMD	ChPT	ChPT (extrapolated)
C_{22}^{Wr}	$\frac{3}{64M_\rho^2\pi^2} \simeq 8.01$	$\begin{cases} 6.52 \pm 0.78 \\ 5.07 \pm 0.71 \end{cases}$	
C_{13}^{Wr}	$-\frac{15}{128M_\rho^2\pi^2} \simeq -20.0$	-74.09 ± 55.89	-8.44 ± 69.9
C_{14}^{Wr}	$-\frac{9}{2} \frac{1}{128M_\rho^2\pi^2} \simeq -6.01$	29.99 ± 11.14	0.72 ± 15.3
C_{15}^{Wr}	$\frac{3}{2} \frac{1}{128M_\rho^2\pi^2} \simeq 2.00$	-25.30 ± 23.93	-3.10 ± 28.6

Table 6: VMD & chiral predictions in MeV^{-2} .

Two equations can be extracted from the $\gamma 3\pi$ amplitude:

$$-C_{13}^{Wr} + C_{14}^{Wr} + C_{15}^{Wr} = \frac{12}{128M_\rho^2\pi^2} \quad (100)$$

$$C_{14}^{Wr} + C_{15}^{Wr} = -\frac{3}{128m_\rho^2\pi^2} \quad (101)$$

From $\eta\gamma\pi\pi$ we get:

$$2C_{15}^{Wr} - 4C_{14}^{Wr} + C_{13}^{Wr} = \frac{3}{64M_\rho^2\pi^2} \quad (102)$$

$$2C_{14}^{Wr} - C_{13}^{Wr} = \frac{3}{64M_\rho^2\pi^2} \quad (103)$$

Exactly the same two equations follow from K_{e4} . There are three independent equations since (102) & (103) can be combined to give (100). In fact, the situation is worse - (101) originates in mass terms produced by kinematical factors. In the derived VMD Lagrangian, approximations have been made removing some of these terms. This means that (101) is subject to corrections that will alter the numerical value somewhat. Only (102) & (103) are exact predictions of the VMD model.

$3/64M_\rho^2\pi^2 \approx 8.0 \times 10^{-9} \text{ MeV}^{-2}$ and evaluating the lefthand side of (102) & (103) using the values in table 3, we obtain $2C_{15}^{Wr} - 4C_{14}^{Wr} + C_{13}^{Wr} \approx (-244.7 \pm 148.4) \times 10^{-9} \text{ MeV}^{-2}$ and $2C_{14}^{Wr} - C_{13}^{Wr} \approx (134.1 \pm 78.17) \times 10^{-9} \text{ MeV}^{-2}$. Using the results of extrapolation in table 4 gives $(-17.52 \pm 188.3) \times 10^{-9} \text{ MeV}^{-2}$ and $(9.88 \pm 100.5) \times 10^{-9} \text{ MeV}^{-2}$ respectively - in much better agreement with the VMD prediction.

Including (101), we can solve for coefficients 13-15. The coefficient values that can be extracted using VMD comparison and the respective chiral predictions are displayed in table 6 in units of 10^{-9} MeV^{-2} .

The values for C_{13}^{Wr} , C_{14}^{Wr} & C_{15}^{Wr} are not great, but we have to remember that coefficients 13-14 also has a part proportional to mass terms that VMD cannot predict. By contrast, C_{22}^{Wr}

is only proportional to k^2 and there VMD does fine. The values obtained by extrapolation are compatible with the VMD predictions.

Of course, the larger the momenta is in the experiment, the more dominant the terms with coefficients connected to the kinematical dependence will be, making the VMD parts increasingly significant.

The shortcomings of the VMD model is illustrated by the plots in figure 7, showing the respective form factors normalized to 1 (with the exception of K_{e4}). The top left plot is for the $\pi^+\gamma e^+\nu$ decay, where the upper plane represents the VMD prediction and the lower one the result from ChPT. Here the influence from the mass term proportional to C_7^{Wr} is very small and C_{22} dominates, so the VMD prediction is well within the error limits.

In the top right plot (for the $K^+\gamma e^+\nu$), the effect of mass terms is more dramatic. Both coefficients C_7^{Wr} & C_{11}^{Wr} are active and bring down the ChPT prediction considerably. The middle plane shows the effect of removing these terms, aligning the ChPT with the VMD prediction.

In the lower left graph (showing $\pi^0(\eta)\gamma\gamma^*$) we see that the effect of mass terms is hardly noticeable for the pion decay. Removing the C_7^{Wr} term from the $\pi^+\gamma\gamma^*$ amplitude does not produce a visibly different result. In the $\eta\gamma\gamma^*$ decay, both C_7^{Wr} and C_8^{Wr} are active, and become augmented by the eta mass. Removing these shifts the curve considerably towards the VMD prediction. The error bars represent the error due to the kinematical term. From looking at the graphs, we can conclude that the pion processes $\pi^+\gamma e\nu$ & $\pi^0\gamma\gamma^*$ are well predicted by VMD, as they are relatively unaffected by the mass terms. Similarly for $\gamma 3\pi$ & $\eta\gamma 2\pi$, VMD does better when only pions are involved. This is because the presence of the η (or K^+ for that matter) induces a greater mass term contribution.

The lower right graph is for the K_{e4} process, where the chiral prediction (solid line) has been extracted using equations from K_{e4} & $\gamma 3\pi$. K_{e4} produces 6 equations and is the major contributor to the predicted form factor. Removing mass terms shifts the ChPT towards the VMD prediction. The solutions in table 3, using all available data, does not produce the same slope as VMD. The possible statistical fluke in the high end of the spectrum is responsible for this, and can only be eliminated by future experiments. Ignoring the fluke by extrapolation, produces a slope similar to VMDs. And if we then remove the mass terms, we get almost perfect correspondence.

12.5 CQM Comparison

With the Lagrangians of appendix B, the corresponding $\mathcal{O}(p^6)$ results from the chiral constituent quark model can be calculated and subsequently compared with the ChPT predictions of table 3. First of all, we need to extract a value for the constituent quark mass - m_Q . We proceed as in [3], making use of the $M \rightarrow \gamma\gamma$ prediction and experimental slope parameters [24]. Setting $R_\mu = L_\mu = eQA_\mu$ in $\Gamma^-(a_3)$, then performing the calculation and adding lowest order (WZW) amplitude gives:

$$A_{M \rightarrow \gamma\gamma}^{CQM} = \frac{ie^2}{4\pi^2 F_M} C_M \varepsilon^{\mu\nu\alpha\beta} \varepsilon_\mu k_\nu \varepsilon_\alpha^* k_\beta^* \left(1 + \frac{k^{\star 2}}{12m_Q^2} \right) \quad (104)$$

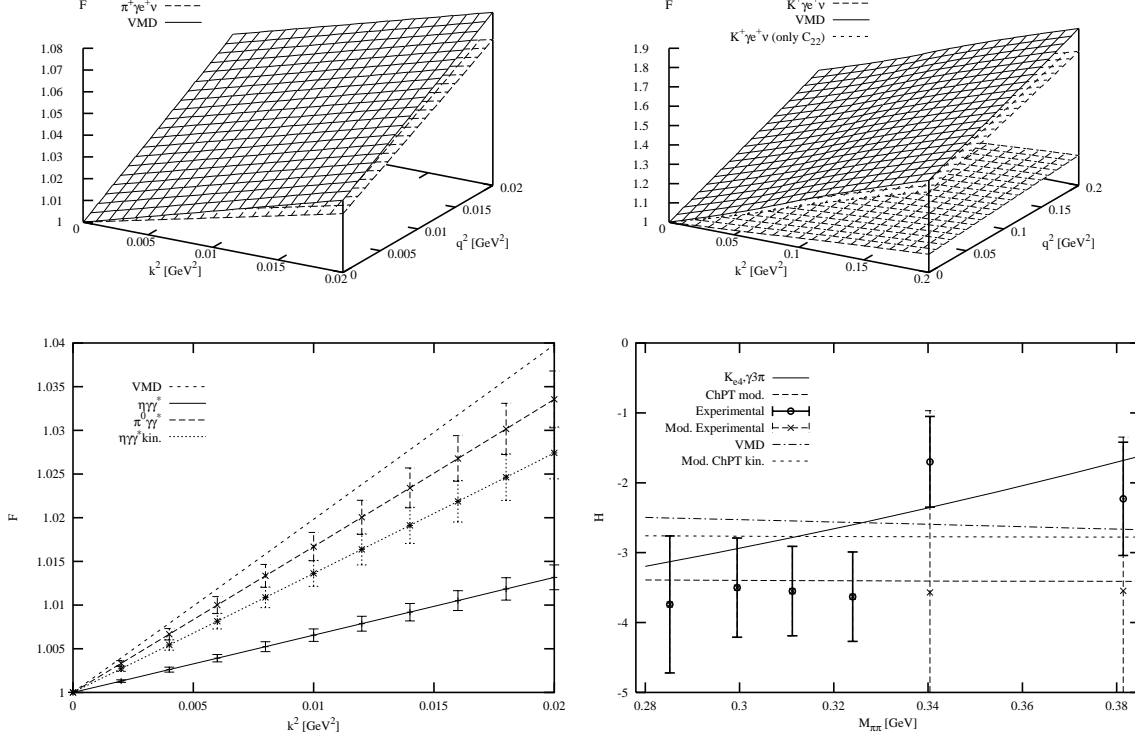


Figure 7: *Form factors.*

where $C_\pi = 1$ & $C_{\eta_8} = 1/\sqrt{3}$. Taking an average of the pole parameters from [24] and using (93) to calculate the slope, we get

$$\begin{cases} \Lambda_{\pi^0} = 776 \pm 38 \text{ MeV} \\ \Lambda_\eta = 774 \pm 39 \text{ MeV} \end{cases} \Rightarrow \langle \Lambda \rangle = 775 \pm 39 \text{ MeV}$$

$$\frac{1}{12m_Q^2} = \frac{1}{\langle \Lambda \rangle^2} \Rightarrow m_Q = \frac{\langle \Lambda \rangle}{\sqrt{12}} \simeq 224 \pm 12 \text{ MeV}$$

Comparing with the $\mathcal{O}(p^6)$ expression in table 5 gives $m_Q = m_\rho/\sqrt{12} \simeq 222 \text{ MeV}$, in excellent agreement with the empirically derived value. Since we are using the same experimental data to fix m_Q that we use to predict the chiral coefficients, we cannot compare the two approaches in the $M \rightarrow \gamma\gamma$ case. Using $m_Q = m_\rho/\sqrt{12}$, will of course give the same C_{22}^{Wr} prediction as VMD. Note that no mass parameters appear in (104). Unfortunately, in deriving the CQM Lagrangian, some mass terms have been approximated away, as they do not alter the end result notably. CQM is in principle able give us predictions for all mass terms. We just have to remember that the equations derived by comparing with these are subject to small corrections.

Table 7 shows the CQM $\mathcal{O}(p^6)$ amplitudes, with the same prefactors as in the ChPT case.

The π^+ and the K^+ decays give the same (exact) prediction for $C_{22}^{Wr} = 1/512m_Q^2\pi^2 \simeq 3.94 \times 10^{-9} \text{ MeV}^{-2}$. It seems that the VMD prediction overestimates the C_{22}^{Wr} value, whereas

<i>Process:</i>	<i>Amplitude:</i>	<i>Lagrangian:</i>
$\pi^0 (\eta) \rightarrow \gamma \gamma^*$	$\frac{k^{*2}}{12m_Q^2}$	$\Gamma^- (a_3)$
$\pi^+ \rightarrow \gamma e^+ \nu$	$\frac{1}{48m_Q^2}(-m_{\pi^+}^2 + 2q^2 + 2k^2)$	$\Gamma^- (a_3)$
$K^+ \rightarrow \gamma e^+ \nu$	$\frac{1}{48m_Q^2}(-m_{K^+}^2 + 3q^2 + 3k^2)$	$\Gamma^- (a_3)$
$\pi^0 \rightarrow \gamma \pi^+ \pi^-$	$\frac{k^2}{6m_Q^2}$	$\Gamma^- (a_4)$
$\eta \rightarrow \gamma \pi^+ \pi^-$	$\frac{1}{30m_Q^2}[8m_\pi^2 - 2m_\eta^2 + 12p_+p_- + 3k^2]$	$\Gamma^- (a_4)$
$K^+ \rightarrow \pi^+ \pi^- e^+ \nu$	$\frac{1}{30m_Q^2}[m_K^2 - m_\pi^2 - 6qp_+ + 3q^2]$	$\Gamma^- (a_4)$

Table 7: *CQM* $\mathcal{O}(p^6)$ amplitudes.

CQM underestimates it by roughly the same amount. Both models do equally well with respect to ChPT.

Comparing the mass terms we get the (inexact) value $C_7^{Wr} \simeq 5.10 \times 10^{-10} \text{MeV}^{-2}$, from the π^+ decay. This can then be used in the K^+ amplitude to get $C_{11}^{Wr} \simeq -1.44 \times 10^{-12} \text{MeV}^{-2}$, which is a bit too small to be taken seriously.

Comparing kinematical terms, $\eta\gamma\pi\pi$ & K_{e4} both give the same two equations.

$$2C_{14}^{Wr} - C_{13}^{Wr} = \frac{2}{5} \frac{1}{128m_Q^2\pi^2} \simeq 6.31 \times 10^{-9} \text{MeV}^{-2} \quad (105)$$

$$2C_{15}^{Wr} - 4C_{14}^{Wr} + C_{13}^{Wr} = \frac{4}{5} \frac{1}{128m_Q^2\pi^2} \simeq 1.26 \times 10^{-8} \text{MeV}^{-2} \quad (106)$$

$\gamma 3\pi$ gives one equation that offers no additional constraints. Equations (105) & (106) are of the exact same form as the VMD predictions (102) & (103), and the predicted value of the RH side lies in between ($8.0 \times 10^{-9} \text{MeV}^{-2}$) those of CQM.

Turning to the mass terms, we get one equation from $\gamma 3\pi$, which can be reconstructed with the two equations from $\eta\gamma\pi\pi$. These are:

$$-6C_{36}^{Wr} + 2C_{14}^{Wr} + C_{13}^{Wr} = \frac{4}{15} \frac{1}{128m_Q^2\pi^2} \quad (107)$$

$$-3C_{36}^{Wr} + C_5^{Wr} + 2C_4^{Wr} - 2C_{14}^{Wr} + C_{13}^{Wr} = \frac{8}{15} \frac{1}{128m_Q^2\pi^2} \quad (108)$$

with $C_{36}^{Wr} \equiv C_3^{Wr} - C_6^{Wr}$. Two additional equations follow from comparing mass terms in K_{e4} :

$$C_2^{Wr} + C_4^{Wr} - C_{14}^{Wr} = \frac{1}{15} \frac{1}{128\pi^2 m_Q^2} \quad (109)$$

$$-C_2^{Wr} + C_4^{Wr} + C_5^{Wr} - C_{15}^{Wr} = -\frac{1}{15} \frac{1}{128\pi^2 m_Q^2} \quad (110)$$

If we wish to solve for the chiral coefficients using the (inexact) predictions from the mass terms (eq. (107)-(110)), we must make additional assumptions. One approach is to parametrize the solution of the system of equations (105)-(110) in terms of (for example) C_{15}^{Wr} & C_4^{Wr} , and

<i>Process:</i>	CQM	CQM (extrapolation)
$\pi^+ \rightarrow \gamma e^+ \nu$	$C_7^{Wr} \simeq 0.51 \pm 0.06$ $C_{22}^{Wr} \simeq 3.94 \pm 0.43$	
$K^+ \rightarrow \gamma e^+ \nu$	$C_{11}^{Wr} \simeq -0.00143 \pm 0.03$ $C_{22}^{Wr} \simeq 3.94 \pm 0.43$	
$\gamma 3\pi, \eta \gamma \pi \pi \text{ \& } K_{e4}$	$C_2^{Wr} \simeq 4.96 \pm 9.70$ $C_{36}^{Wr} \simeq 5.07 \pm 5.07$ $C_4^{Wr} \simeq 6.32 \pm 6.09$ $C_5^{Wr} \simeq 33.05 \pm 28.66$ $C_{13}^{Wr} \simeq 14.15 \pm 15.22$ $C_{14}^{Wr} \simeq 10.23 \pm 7.56$ $C_{15}^{Wr} \simeq 19.70 \pm 7.49$	$C_2^{Wr} \simeq -0.074 \pm 13.3$ $C_{36}^{Wr} \simeq -2.14 \pm 6.54$ $C_4^{Wr} \simeq -0.55 \pm 9.05$ $C_5^{Wr} \simeq 34.51 \pm 41.13$ $C_{13}^{Wr} \simeq -7.46 \pm 19.62$ $C_{14}^{Wr} \simeq -0.58 \pm 9.77$ $C_{15}^{Wr} \simeq 8.89 \pm 9.72$

Table 8: *CQM & chiral predictions in MeV^{-2} .*

then vary it freely with the constraint that the solution should stay as close to the ChPT result as possible, given the error limits. Table 8 displays the results of applying this procedure on the full ChPT and extrapolated ChPT result, respectively. Looking at figure 8, showing the ChPT along with CQM and VMD predicted coefficients in units of 10^{-9} MeV^{-2} , we see that the best result is obtained by extrapolation. The quoted CQM errors arise from the constraints in the fitting process and from the constituent quark mass error, and are not intrinsic to the model.

Figure 9 shows the chiral and CQM form factor predictions for $\pi^+ \gamma e^+ \nu$ (top left), $K^+ \gamma e^+ \nu$ (top right), $\gamma 3\pi$ (bottom left) and K_{e4} (bottom right). For π^+ (K^+) $\gamma e^+ \nu$ CQM does slightly better than VMD, but fails to predict the mass terms in the $K^+ \gamma e^+ \nu$ case. In the $\gamma 3\pi$ process, CQM & VMD fit well with the coefficients obtained by extrapolating, less so with the full data set. In the K_{e4} , both VMD & CQM predict roughly the same form factor.

13 Conclusions & Outlook

To gain insight into the physics leading to the chiral Lagrangian, it is vital to chart the anomalous territory. Ultimately, we hope to arrive at a complete standard model derivation, capable of predicting all the chiral parameters. Going through the ChPT theory up to the anomalous $\mathcal{O}(p^6)$ Lagrangian, we are faced with a large number of coefficients, that can be empirically determined through comparison with available experimental data. As much information as possible is extracted using the amplitudes calculated for a number of different anomalous processes. The extracted values then allow us to test the predictions of two other models for the C_i^{Wr} s: the vector meson dominance and the chiral constituent quark model.

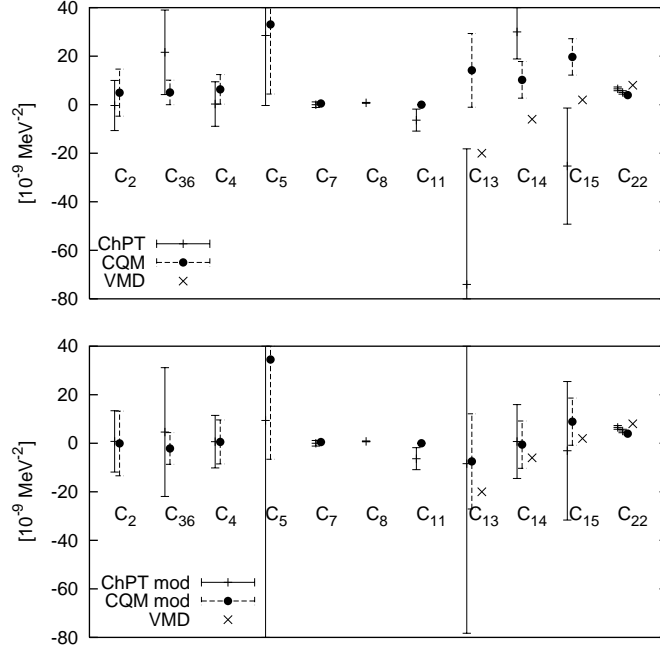


Figure 8: *Chiral coefficients (bottom: using extrapolation).*

VMD does very well in predicting the coefficients that are connected to kinematical factors, but fails to fully predict those that do not vanish in the low energy limit. Here the CQM does better, and gives reasonable predictions for all coefficients.

To improve the accuracy in gauging the validity of these models, and to reduce the errors of the C_i^{Wr} s further, more detailed experiments must be made, probing the anomalous sector. Many such experiments are in the planning stages today, e.g. the Primex precision π^0 lifetime measurements at Jefferson laboratories.

References

- [1] J. Wess and B. Zumino, "Consequences of the anomalous Ward identities", *Phys. Lett.* **B37** (1971) 95
- [2] E. Witten, "Global aspects of current algebra", *Nucl. Phys.* **B223** (1983) 422
- [3] J. Bijnens "Chiral Perturbation Theory and Anomalous Processes", *Int. J. Mod. Phys.* **A Vol. 8 No. 18** (1993)
- [4] G.C. Callan, S. Coleman, J. Wess & B. Zumino, *Phys. rev.* **177** , 2239; 2247 (1969)
- [5] Gilberto Colangelo & Gino Isidori, "An Introduction to ChPT", hep-ph/0101264
- [6] J. Gasser and H. Leutwyler, *Nucl. Phys.* **B250** 465 (1985)
- [7] Michael E. Peskin, Daniel V. Schroeder, "An Introduction to Quantum Field Theory", Westview press (1995), 661

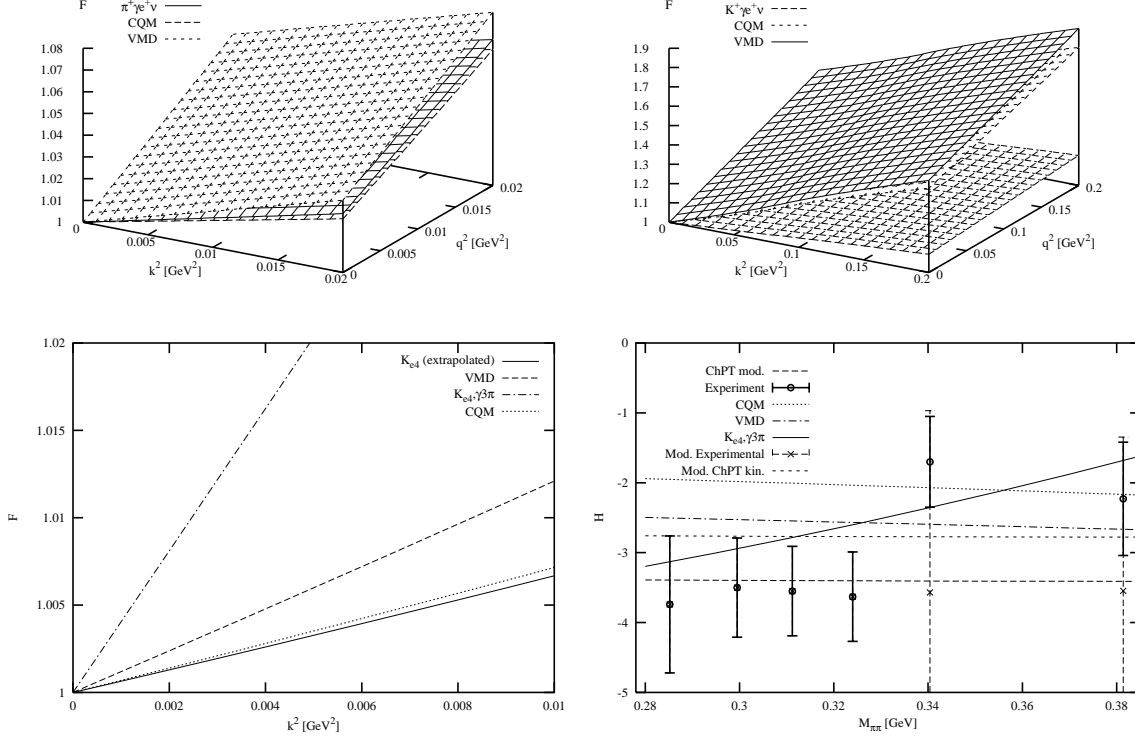


Figure 9: *Form factors.*

- [8] M. Gell-Mann, R. Oakes & B. Renner , "Behaviour of current divergences under $SU(3) \times SU(3)$ ", *Phys. Rev.* **175**, 2195 (1968)
- [9] J. F. Donoghue, E. Golowich, B. R. Holstein, "Dynamics of the Standard Model", Cambridge University Press (1996)
- [10] J. Gasser and H. Leutwyler, *Ann. Phys (N.Y.)* **158**, 142 (1984)
- [11] J. Bijnens, L. Girlanda and P. Talavera, "The Anomalous Chiral Lagrangian of order p^6 ", *Eur. Phys. J.* **C23**, 539-544
- [12] F. J. Gilman and R. Kauffman " η - η' mixing angle" *Phys. Rev.* **D36**, 2761 (1987)
- [13] K. Fujikawa, "Path integral measure for gauge invariant field theories", *Phys. Rev.* **D23**, 2262 (1979)
- [14] S. L. Adler, *Phys. Rev.* **177**, 2426 (1969)
- [15] J. S. Bell and R. Jackiw, *Nuovo Cim.* **A60**, 47 (1969)
- [16] S. L. Adler and W. A. Bardeen, "Absence of higher order corrections in the anomalous axial-vector divergence equation" *Phys. Rev.* **182**, 1517 (1969)
- [17] J. Steinberger, , 1180 (1949)

- [18] K. Hagiwara et al. (Particle Data Group) *Phys. Rev.* **D66**, 010001 (2002), (URL: <http://pdg.lbl.gov>)
- [19] S. Weinberg, "Phenomenological Lagrangians", *Physica* **A96**, 327 (1979)
- [20] J. Bijnens, A. Bramon and F. Cornet *Phys. Rev. Lett.* **61**, 1453 (1988)
- [21] Ll. Ametller, J. Bijnens, A. Bramon and F. Cornet, "Semileptonic π and K decays and the chiral anomaly at one-loop", *Phys. Lett.* **B303**, 140 (1993)
- [22] M. Bando, T. Kugo and K. Yamawaki, *Phys. Rep.* **164**, 217 (1988)
- [23] R. D. Ball, *Phys. Rep.* **182**, 1 (1989)
- [24] CLEO Collaboration, "Measurements of the meson-photon transition form factors of light pseudoscalar mesons at large momentum transfer", CLNS 97/1477, CLEO 97-7, hep-ex/9707031 (1998)
- [25] S. Pislak et al., "New measurement of K_{e4}^+ decay and the s-wave scattering length a_0^0 ", *Phys. Rev. Lett.* Vol. **87**, No. **22** (2001)
- [26] A. Bramon, J. Bijnens and F. Cornet, "Chiral Perturbation Theory for γPPP Processes", presented at Daphne Workshop 1990; UAB-FT-263/91, UG-FT-15/91
- [27] J. Bijnens, A. Bramon and F. Cornet, *Phys. Rev. Lett.* **61**, 1453 (1988); J. Donoghue and D. Wyler, *Nucl. Phys* **B316**, 289 (1989)
- [28] Y.N. Antipov et al., *Phys. Rev.* **D36**, 21 (1987)

Acknowledgements

Johan Bijnens - *Thank you* Hans for being the best tutor I could possibly hope for. I would also like to thank all other experimental and theoretical physicists, upon who's hard work this thesis is based on. And of course my mother, for her invaluable moral support.

A One-loop Corrections

Process:	Amplitude:
$\pi^0 \rightarrow \gamma e^+ e^-$	$\frac{1}{4\pi^2} \frac{e^3}{F_\pi} \varepsilon^{\mu\nu\alpha\beta} \varepsilon_\mu k_\nu \frac{\bar{e} \gamma_\alpha e}{k^{*2}} k_\beta^* \frac{1}{32\pi^2 F^2} \times$ $\left\{ -\frac{1}{3} k^{*2} \left(\log \frac{m_K^2}{\mu^2} + \log \frac{m_\pi^2}{\mu^2} \right) + \frac{10}{9} k^{*2} + \frac{4}{3} [F(k^{*2}, m_\pi^2) + F(k^{*2}, m_K^2)] \right\}$
$\eta \rightarrow \gamma e^+ e^-$	$\frac{e^3}{4\sqrt{3}\pi^2 F_\eta} \varepsilon^{\mu\nu\alpha\beta} \varepsilon_\mu k_\nu \frac{\bar{e} \gamma_\alpha e}{k^{*2}} k_\beta^* \frac{1}{32\pi^2 F^2} \times$ $\left\{ -\frac{1}{3} k^{*2} \left(\log \frac{m_K^2}{\mu^2} + \log \frac{m_\pi^2}{\mu^2} \right) + \frac{10}{9} k^{*2} + \frac{4}{3} [F(k^{*2}, m_\pi^2) + F(k^{*2}, m_K^2)] \right\}$

$\pi^+ \rightarrow \gamma e^+ \nu$	$\frac{eG_F \cos \theta}{8\pi^2 F_\pi} \varepsilon^{\mu\nu\alpha\beta} l_\mu q_\nu \varepsilon_\alpha k_\beta \frac{1}{32\pi^2 F^2} \times$ $\{-4m_\pi^2 \ln \frac{m_\pi^2}{\mu^2} - 4m_K^2 \ln \frac{m_K^2}{\mu^2} + 4I(q^2, m_\pi^2, m_\pi^2) + 4I(k^2, m_K^2, m_K^2)\}$
$K^+ \rightarrow \gamma e^+ \nu$	$\frac{eG_F \sin \theta}{8\pi^2 F_K} \varepsilon^{\mu\nu\alpha\beta} l_\mu q_\alpha \varepsilon_\beta k_\beta \times$ $\frac{1}{32\pi^2 F^2} \{-\frac{7}{2}m_\pi^2 \ln \frac{m_\pi^2}{\mu^2} - 3m_K^2 \ln \frac{m_K^2}{\mu^2} - \frac{3}{2}m_\eta^2 \ln \frac{m_\eta^2}{\mu^2}$ $+ 4I(k^2, m_\pi^2, m_\pi^2) + 2I(q^2, m_K^2, m_\pi^2) + 2I(q^2, m_K^2, m_\eta^2)\}$
$\gamma \pi^0 \pi^+ \pi^-$	$i \frac{1}{4\pi^2} \frac{e}{F_\pi^3} \varepsilon^{\mu\nu\alpha\beta} \varepsilon_\mu p_\nu p_\alpha p_\beta \times$ $\frac{1}{96\pi^2 F^2} \{-(p_{01}^2 + p_{02}^2 + p_{12}^2) \log \frac{m_\pi^2}{\mu^2} + \frac{5}{3}(p_{01}^2 + p_{02}^2 + p_{12}^2)$ $+ 4[F(m_\pi^2, p_{01}^2) + F(m_\pi^2, p_{02}^2) + F(m_\pi^2, p_{12}^2)]\}$
$\gamma \eta_8 \pi^+ \pi^-$	$-i \frac{1}{4\pi^2 \sqrt{3}} \frac{e}{F_\pi^2 F_{\eta_8}} \varepsilon^{\mu\nu\alpha\beta} \varepsilon_\mu p_\nu p_\alpha^+ p_\beta^- \times$ $\frac{1}{32\pi^2 F^2} \{-(4m_\pi^2 + \frac{1}{3}p_{12}^2) \log \frac{m_\pi^2}{\mu^2} + (4m_K^2 - \frac{2}{3}p_{12}^2) \log \frac{m_K^2}{\mu^2}$ $+ \frac{5}{3}p_{12}^2 + \frac{4}{3}F(m_\pi^2, p_{12}^2) + \frac{8}{3}F(m_K^2, p_{12}^2)\}$
$K^+ \rightarrow \pi^+ \pi^- e^+ \nu$	$\frac{G_F \sin \theta}{4\pi^2 F_\pi^2 F_K} \varepsilon^{\mu\nu\alpha\beta} l_\mu q_\nu p_\alpha^+ p_\beta^- \times$ $[\frac{1}{32\pi^2 F^2} \{-\frac{11}{2}m_\pi^2 \ln \frac{m_\pi^2}{\mu^2} - 5m_K^2 \ln \frac{m_K^2}{\mu^2} - \frac{3}{2}m_\eta^2 \ln \frac{m_\eta^2}{\mu^2}$ $+ 2I((p^+ + p^-)^2, m_\pi^2, m_\pi^2) + I((p^+ + p^-)^2, m_K^2, m_K^2)$ $+ 2I((p^- + q)^2, m_K^2, m_\pi^2) + I((p^- + q)^2, m_K^2, m_\eta^2)$ $+ 3I(q^2, m_K^2, m_\pi^2) + 3I(q^2, m_K^2, m_\eta^2)\}]$
$K^+ \rightarrow \pi^0 \pi^0 e^+ \nu$	$\frac{G_F \sin \theta}{4\pi^2 F_K F_\pi^2} \varepsilon^{\mu\nu\alpha\beta} l_\mu q_\nu p_\alpha p'_\beta \times$ $[\frac{1}{32\pi^2 F^2} \{-I((q + p)^2, m_K^2, m_\pi^2) - \frac{1}{2}I((q + p)^2, m_K^2, m_\eta^2)$ $+ I((q + p')^2, m_K^2, m_\pi^2) + \frac{1}{2}I((q + p')^2, m_K^2, m_\eta^2)\}]$

where

$$\begin{aligned}
F(m^2, x) &\equiv m^2 \left(1 - \frac{x}{4}\right) \sqrt{\frac{x-4}{x}} \log \frac{\sqrt{x} - \sqrt{x-4}}{-\sqrt{x} + \sqrt{x-4}} - 2m^2 \quad ; x \equiv \frac{k^{*2}}{m^2} \\
I(k^2, m_1^2, m_2^2) &\equiv \int_0^1 dx \left[m_1^2 - (m_1^2 - m_2^2)x - x(1-x)k^2 \right] \times \\
&\quad \log \frac{m_1^2 - (m_1^2 - m_2^2)x - x(1-x)k^2}{\mu^2} \\
&= 16\pi^2 \left\{ \frac{m_1^2 - m_2^2 + k^2}{6k^2} iA(m_1^2) + \frac{-m_1^2 + m_2^2 + k^2}{6k^2} iA(m_2^2) \right. \\
&\quad \left. - \frac{(m_1^2 - m_2^2 - k^2)^2 - 4k^2 m_2^2}{6k^2} iB(k^2, m_1^2, m_2^2) - \frac{1}{3}(m_1^2 + m_2^2) + \frac{1}{9}k^2 \right\} \\
iA(m^2) &\equiv \frac{m^2}{16\pi^2} \ln \frac{m^2}{\mu^2} \\
iB(k^2, m_1^2, m_2^2) &\equiv -\frac{1}{16\pi^2} \left(1 - \frac{1}{2} \log \frac{m_1^2 m_2^2}{\mu^4} + \frac{m_2^2 - m_1^2}{2k^2} \log \frac{m_1^2}{m_2^2} - \frac{1}{k^2} u_+ u_- \log \frac{u_+ + u_-}{u_+ - u_-} \right) \\
u_{\pm} &\equiv \sqrt{k^2 - (m_1^2 \pm m_2^2)^2}
\end{aligned}$$

B *CQM Lagrangians*

5 pseudoscalars:

$$\begin{aligned}
\Gamma^-(a_5) &= -\frac{N_c}{32\pi^2} \int d^4x \frac{1}{30} \varepsilon_{\mu\nu\alpha\beta} \\
&\quad \times \text{tr} \left[\left(\Sigma D_\gamma D_\mu \Sigma^\dagger - D_\gamma D_\mu \Sigma \Sigma^\dagger \right) D_\nu (D_\alpha \Sigma^\dagger D_\gamma \Sigma - D_\gamma \Sigma^\dagger D_\alpha \Sigma) D_\beta \Sigma^\dagger \right]
\end{aligned}$$

1 external vector field & 3 pseudoscalars:

$$\begin{aligned}
\Gamma^-(a_4) = & \frac{N_c}{32\pi^2 m_Q^2} \int d^4x \frac{i}{180} \varepsilon_{\mu\nu\alpha\beta} \\
& \text{tr}\{2 \left(D_\gamma r_{\gamma\mu} + \Sigma^\dagger D_\gamma \ell_{\gamma\mu} \Sigma \right) D_\nu \Sigma^\dagger D_\alpha \Sigma D_\beta \Sigma^\dagger \Sigma \\
& -3 \left(D_\gamma r_{\mu\nu} + \Sigma^\dagger D_\gamma \ell_{\mu\nu} \Sigma \right) D_\alpha \Sigma^\dagger D_\gamma \Sigma D_\beta \Sigma^\dagger \Sigma \\
& + r_{\mu\gamma} [20 D_\nu \Sigma^\dagger D_\alpha \Sigma \Sigma^\dagger D_\gamma D_\beta \Sigma - 20 D_\gamma D_\nu \Sigma^\dagger \Sigma D_\alpha \Sigma^\dagger D_\beta \Sigma \\
& - 2 D_\nu \Sigma^\dagger D_\alpha \Sigma D_\gamma D_\beta \Sigma^\dagger \Sigma + 2 \Sigma^\dagger D_\gamma D_\nu \Sigma D_\alpha \Sigma^\dagger D_\beta \Sigma \\
& - 8 D_\nu \Sigma^\dagger \left(\Sigma D_\gamma D_\alpha \Sigma^\dagger - D_\gamma D_\alpha \Sigma \Sigma^\dagger \right) D_\beta \Sigma] \\
& - \ell_{\mu\gamma} [20 D_\nu \Sigma D_\alpha \Sigma^\dagger \Sigma D_\gamma D_\beta \Sigma^\dagger - 20 D_\gamma D_\nu \Sigma \Sigma^\dagger D_\alpha \Sigma D_\beta \Sigma^\dagger \\
& - 2 D_\nu \Sigma D_\alpha \Sigma^\dagger D_\gamma D_\beta \Sigma \Sigma^\dagger + 2 \Sigma D_\gamma D_\nu \Sigma^\dagger D_\alpha \Sigma D_\beta \Sigma^\dagger \\
& - 8 D_\nu \Sigma \left(\Sigma^\dagger D_\gamma D_\alpha \Sigma - D_\gamma D_\alpha \Sigma^\dagger \Sigma \right) D_\beta \Sigma^\dagger] \\
& + 3 r_{\mu\nu} [D_\gamma D_\alpha \Sigma^\dagger \Sigma D_\beta \Sigma^\dagger D_\gamma \Sigma + D_\alpha \Sigma^\dagger D_\gamma D_\beta \Sigma \Sigma^\dagger D_\gamma \Sigma \\
& - D_\gamma \Sigma^\dagger \Sigma D_\gamma D_\alpha \Sigma^\dagger D_\beta \Sigma - D_\gamma \Sigma^\dagger D_\alpha \Sigma \Sigma^\dagger D_\gamma D_\beta \Sigma] \\
& - 3 \ell_{\mu\nu} [D_\gamma D_\alpha \Sigma \Sigma^\dagger D_\beta \Sigma D_\gamma \Sigma^\dagger + D_\alpha \Sigma D_\gamma D_\beta \Sigma^\dagger \Sigma D_\gamma \Sigma^\dagger \\
& - D_\gamma \Sigma \Sigma^\dagger D_\gamma D_\alpha \Sigma D_\beta \Sigma^\dagger - D_\gamma \Sigma D_\alpha \Sigma^\dagger \Sigma D_\gamma D_\beta \Sigma^\dagger] \\
& - 2 D^2 D_\mu \Sigma \{ r_{\nu\alpha} \Sigma^\dagger - \Sigma^\dagger \ell_{\nu\alpha}, \Sigma D_\beta \Sigma^\dagger \} \\
& + 2 D^2 D_\mu \Sigma^\dagger \{ \ell_{\nu\alpha} \Sigma - \Sigma r_{\nu\alpha}, \Sigma^\dagger D_\beta \Sigma \} \\
& + i 2 D_\mu D_\gamma D_\nu \Sigma [2 D_\gamma D_\alpha \Sigma^\dagger \Sigma D_\beta \Sigma^\dagger + 2 D_\beta \Sigma^\dagger \Sigma D_\gamma D_\alpha \Sigma^\dagger \\
& + \Sigma^\dagger D_\gamma D_\alpha \Sigma D_\beta \Sigma^\dagger + D_\beta \Sigma^\dagger D_\gamma D_\alpha \Sigma \Sigma^\dagger] \\
& - i 2 D_\mu D_\gamma D_\nu \Sigma^\dagger [2 D_\gamma D_\alpha \Sigma \Sigma^\dagger D_\beta \Sigma + 2 D_\beta \Sigma \Sigma^\dagger D_\gamma D_\alpha \Sigma \\
& + \Sigma D_\gamma D_\alpha \Sigma^\dagger D_\beta \Sigma + D_\beta \Sigma D_\gamma D_\alpha \Sigma^\dagger \Sigma] \}
\end{aligned}$$

2 external vector fields & 1 pseudoscalar:

$$\begin{aligned}
\Gamma^-(a_3) = & -\frac{N_c}{32\pi^2 m_Q^2} \int d^4x \frac{1}{120} \varepsilon_{\mu\nu\alpha\beta} \\
& \text{tr} \{ 7 \{ D_\gamma r_{\gamma\mu}, r_{\alpha\beta} \} D_\nu \Sigma^\dagger \Sigma \\
& - 7 \{ D_\gamma \ell_{\gamma\mu}, \ell_{\alpha\beta} \} D_\nu \Sigma \Sigma^\dagger \\
& + 2 D_\gamma r_{\gamma\mu} \left(\Sigma^\dagger \ell_{\alpha\beta} D_\nu \Sigma - D_\nu \Sigma^\dagger \ell_{\alpha\beta} \Sigma \right) \\
& - 2 D_\gamma \ell_{\gamma\mu} \left(\Sigma r_{\alpha\beta} D_\nu \Sigma^\dagger - D_\nu \Sigma r_{\alpha\beta} \Sigma^\dagger \right) \\
& + 3 \{ r_{\mu\gamma}, r_{\alpha\beta} \} \left(\Sigma^\dagger D_\gamma D_\nu \Sigma - D_\gamma D_\nu \Sigma^\dagger \Sigma \right) \\
& - 3 \{ \ell_{\mu\gamma}, \ell_{\alpha\beta} \} \left(\Sigma D_\gamma D_\nu \Sigma^\dagger - D_\gamma D_\nu \Sigma \Sigma^\dagger \right) \\
& + 4 \ell_{\mu\gamma} \left(D_\gamma D_\nu \Sigma r_{\alpha\beta} \Sigma^\dagger - \Sigma r_{\alpha\beta} D_\gamma D_\nu \Sigma^\dagger \right) \\
& - 4 r_{\mu\gamma} \left(D_\gamma D_\nu \Sigma^\dagger \ell_{\alpha\beta} \Sigma - \Sigma^\dagger \ell_{\alpha\beta} D_\gamma D_\nu \Sigma \right) \\
& + 2 \ell_{\mu\gamma} \left(D_\nu \Sigma D_\gamma r_{\alpha\beta} \Sigma^\dagger - \Sigma D_\gamma r_{\alpha\beta} D_\nu \Sigma^\dagger \right) \\
& - 2 r_{\mu\gamma} \left(D_\nu \Sigma^\dagger D_\gamma \ell_{\alpha\beta} \Sigma - \Sigma^\dagger D_\gamma \ell_{\alpha\beta} D_\nu \Sigma \right) \\
& - 13 \{ r_{\mu\gamma}, D_\gamma r_{\alpha\beta} \} D_\nu \Sigma^\dagger \Sigma \\
& + 13 \{ \ell_{\mu\gamma}, D_\gamma \ell_{\alpha\beta} \} D_\nu \Sigma \Sigma^\dagger \\
& + [r_{\alpha\beta}, r_{\mu\gamma}] \left(\Sigma^\dagger D_\gamma D_\nu \Sigma + D_\gamma D_\nu \Sigma^\dagger \Sigma \right) \\
& - [\ell_{\alpha\beta}, \ell_{\mu\gamma}] \left(\Sigma D_\gamma D_\nu \Sigma^\dagger + D_\gamma D_\nu \Sigma \Sigma^\dagger \right) \}
\end{aligned}$$